ELSEVIER

Journal of Organometallic Chemistry 630 (2001) 88–103

Journal of Organometallic Chemistry

www.elsevier.com/locate/jorganchem

Regio- and stereoselectivity in long-range asymmetric induction controlled by carbonyliron groups: crystal structures of dicarbonyl-L-[(1,2,3,4,5-η)-1-R-4-methoxycyclohexadienyl]iron(1 +) hexafluorophosphate(1 −) [(R = isopropenyl, L = CO), (R = 1-styryl, L = CO), (R = 1-prop-1-enyl, L = PPh_3)] and tricarbonyl[methyl(2,3,4,5-η)-2-carbomethoxy-2-(4-methoxy-1-(1′-methylethenyl)cyclohexadien-1-yl)ethanoate]iron(0)

Richard D.A. Hudson [a,*], Christopher E. Anson [b], Mary F. Mahon [c], G. Richard Stephenson [d,1]

[a] *Department of Chemistry, University College Dublin, Belfield, Dublin 4, Ireland*
[b] *Institut für Anorganische Chemie, Universität Karlsruhe, Engesserstrasse Geb 30.45, 76131 Karlsruhe, Germany*
[c] *Department of Chemistry, University of Bath, Bath BA2 7AY, UK*
[d] *School of Chemical Sciences, University of East Anglia, Norwich NR4 7TJ, UK*

Received 16 January 2001; received in revised form 6 February 2001

This paper is dedicated to Professor Myron Rosenblum on the occasion of his 75th birthday. One of us, R.D.A.H. had the pleasure and privilege to undertake a period of postdoctoral work in Professor Rosenblum's laboratories at Brandeis University, Waltham, MA, USA, from 1997 to 1999 [1]

Abstract

The synthesis of alkenyl-extended cyclohexadienyliron complexes is described and reactions are reported demonstrating that regio- and stereoselective functionalisation can be controlled by the judicious choice of nucleophile, alkali metal counterion and ligand set at iron. The crystal structures of tricarbonyl[(1,2,3,4,5-η)-1-(1′-methylethenyl)-4-methoxycyclohexadienyl]iron(1 +) hexafluorophosphate(1 −), tricarbonyl[(1,2,3,4,5-η)-1-(ethenyl-1′-phenyl)-4-methoxycyclohexadienyl]iron(1 +) hexafluorophosphate(1 −), (*E*)-dicarbonyl[(1,2,3,4,5-η)-1-(2′-methylethenyl)-4-methoxycyclohexadienyl]triphenylphosphineiron(1 +) hexafluorophosphate(1 −), tricarbonyl[methyl(2,3,4,5-η)-2-carbomethoxy-2-(4-methoxy-1-(1′-methylethenyl)cyclohexadien-1-yl)ethanoate]-iron(0), are reported. The stereochemical course of a long-range relay of chirality controlled by the carbonyliron group is proven.

Keywords: Tricarbonyliron; Cyclohexadienyliron; Chiral; Stereoselective; Regioselective

1. Introduction

Electrophilic transition metal complexes have powerful control effects when employed in combination with nucleophiles in organic synthesis [2]. The metal centre exerts complete stereocontrol and for direct addition the nucleophile approaches *trans* to the metal. In stochiometric systems, while it is desirable in terms of efficiency for the metal to be used several times to control a sequence of bond-forming reactions, in practice (particularly with cyclic ligands) there are severe limitations to the scope of reaction sequences in which the metal moves through the ligand by a series of η^5–η^4 (nucleophile addition) and η^4–η^5 (reactivation

* Corresponding author.
E-mail address: richard.hudson@ucd.ie (R.D.A. Hudson).
[1] *Also corresponding author.

0022-328X/01/$ - see front matter
PII: S0022-328X(01)00734-3

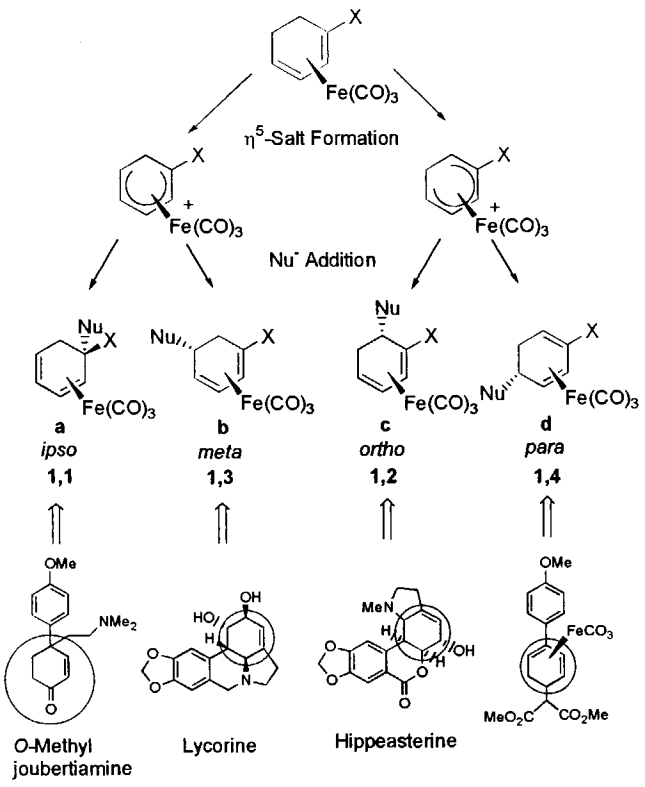

Fig. 1. (a) 1,1-, (b) 1,2-, (c) 1,3- and (d) 1,4-regioisomeric substitution patterns from reaction sequences that employ one iteration of η^5-salt formation and nucleophile addition with diene and dienyl working ligands. Examples of natural product synthesis illustrating these substitution patterns.

of electrophilicity) steps. Recent progress with acyclic structures [3], however, illustrates the potential of these procedures to effect repeated stereocontrol to form a series of chiral centres in reactions that exploit leaving groups to reform the η^5-series. Similar approaches using η^4 and η^5 complexes in six membered rings [4] are clearly limited to a maximum of two chiral centres. In applications such as these, one of the ligands becomes incorporated into the final target structure. This ligand is termed the 'working ligand' [5] and, in an efficient synthetic route, its substituents should match the desired substitution pattern of the corresponding section of the target structure. The analysis of the reactivity properties (particularly regio- and stereoselectivity) of the working ligand is thus an important stage in the design process during the planning of a synthetic route.

Even a simple sequence of two metal-mediated steps directly at the working ligand can offer versatile patterns for controlled sequential bond-formation (Fig. 1), with 1,1- [6,7], 1,2- [8], 1,3- [9] and 1,4- [10] structures all accessible. The challenge in recent years has been to develop processes that allow selective access to each of these forms and now in many cases, the required pattern of reactivity has been demonstrated in actual target oriented routes. The 1,1-pattern has been employed in the synthesis of *O*-methyl joubertiamine [6] and a formal total synthesis of lycoramine [7]. The key is to exploit the directing effect of C-1 alkoxy substituents to ensure a leaving group is in place at the site of the first nucleophile addition, so that this again becomes a terminus of the dienyl moiety when this is reformed in preparation for a reaction with the second nucleophile. Access to the 1,2-pattern is achieved, simply by moving the position of the leaving group from C-1 to C-6 and this approach has allowed the construction of the ABC ring portion of hippeastrine [8]. Rearranging the substitution pattern to the 1,2-dimethoxycyclohexadienyl isomer gives access to the 1,3-pathway, which has been demonstrated in a series of reactions that place C_2 and aryl substituents in positions corresponding to the main structural features of the lycorine skeleton [9]. A methoxy group at C-2 is used for the 1,4-pattern [10] (Fig. 1).

These concepts may be extended by introducing a vinyl group at the terminus of the dienyl system which is activated towards nucleophilic attack in a remote sense by the working ligand (Fig. 2). In this paper, we report results that demonstrate long-range control effects, establishing iron-controlled relative stereochemistry at three chiral centres. This approach allows the metal to reach out from the hapto-bound portion of the ligand to promote electrophilicity and impart stereo-

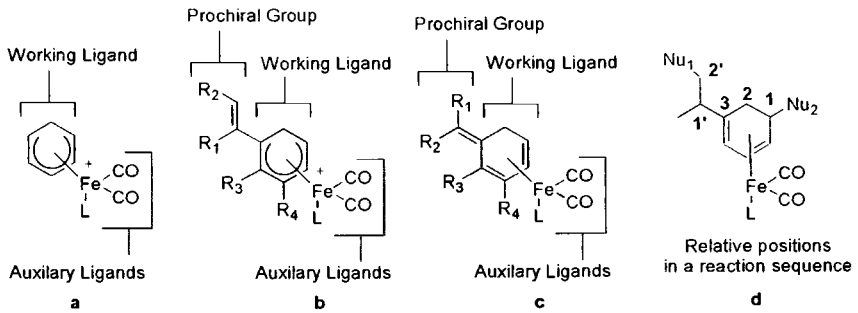

Fig. 2. (a) Illustration of the concepts of 'working' and auxiliary ligands in synthesis design. (b) and (c) An unsymmetrical working ligand forms a chiral complex which can influence stereochemistry at nearby prochiral organic functional groups. (d) The relative positions in a reaction sequence.

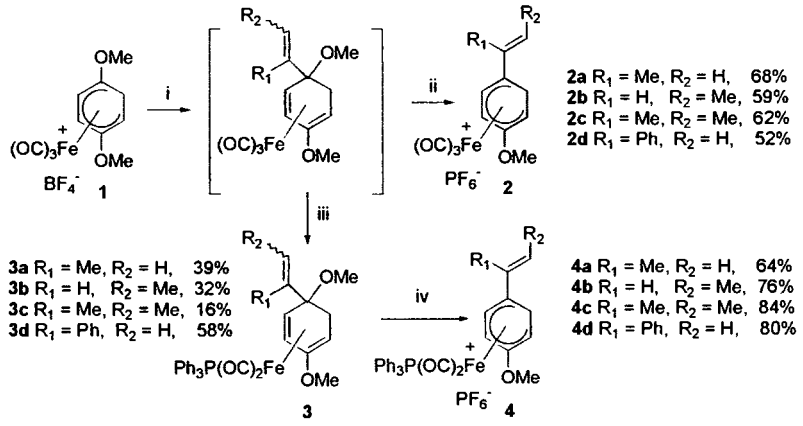

Scheme 1. *Reagents and conditions*: (1) vinyllithium, THF, −100°C; (2) HPF_6, Ac_2O, 0°C; (3) Me_3NO, PPh_3, acetone; (4) HPF_6, Ac_2O, 0°C.

control. In this way, metals moving within cyclohexadiene/cyclohexadienyl ligands can control many chiral centres as far as two atoms out from the working ligand itself. There is considerable precedence for the use of electrophilic metal complexes to activate alkenes. Early work by Rosenblum established that (1,2-η)-butadiene complexes of $Fe(CO)_2Cp^+$ could be electrophilic at C-4 [11]. Cuprates or Grignards were shown to add regioselectively to the remote terminus in good yields and in an extension of this concept both enamines and dialkyl malonates were found to react similarly [12]. He also demonstrated that the uncomplexed double bond in the η^5-cycloheptatrienyliron system is also activated towards nucleophilic attack [13].

2. Results and discussion

2.1. Synthesis of *2* and *4*

Complexes **2** were synthesised by the addition of alkenyllithium reagents to the dimethoxy-substituted complex **1** followed by the removal of the allylic OMe group from the partially purified adducts to afford the salts in good yield on a multigram scale. The corresponding phosphine analogues **4** were prepared by a ligand exchange reaction (CO to PPh_3) on the neutral methoxy adducts followed by salt formation as before. Complexes **2b** and **4b** were formed in stereoconvergent syntheses, by addition of the stereo-undefined *E*/*Z* mixture of lithiopropenes (formed from the corresponding mixture of bromopropenes) to **1** followed by serendipitous equilibration of the alkene adducts during the demethoxylation step (Scheme 1).

2.2. X-ray structures of *2a*, *2d* and *4b*

Compounds **2a**, **2d** and **4b** afforded single crystals suitable for X-ray analysis and Ortex [14] diagrams of the molecular structures are presented in Figs. 3–5. Selected bond lengths and angles are presented in Table 1 (see Table 3 for crystallographic data and structure refinement). In general, the features of the structures do not differ greatly from other substituted tricarbonyliron cyclohexadienyl compounds reported in the literature [15]. The carbonyl ligands do not differ in bond lengths or angles within or between complexes **2a** and **2d** (representative examples are: **2a** Fe(1)–C(2) = 1.818(9); C(1)–O(1) = 1.121(9) Å; C(1)–Fe(1)–C(2) = 96.5°; **2d** Fe(1)–C(2) = 1.830(8); C(1)–O(1) = 1.127(11) Å; C(1)–Fe(1)–C(3) = 96.1°) and are similar to the literature values [15]. Dicarbonyl complex **4d** exhibits slightly shortened Fe to carbonyl bond lengths (Fe(1)–C(1) = 1.781(6); Fe(1)–C(2) = 1.779(7) Å) and a slightly wider angle between them (C(1)–Fe(1)–C(2) = 99.9°) with respect to **2a** and **2d**, indicating more of the back bonding from the metal to phosphine ligand than steric compression. Of course, this balance of π-bonding effects is also seen in the carbonyl region of the IR spectra (cm^{-1}): *ν*(CO) **2a** 2108, 2067, 2038; **2d** 2107, 2058, 2035; **4b** 2032, 1984. The $Fe(CO_2)L$ groups are orientated such that one of the carbonyl ligands eclipses the methylene group and the tripod adopts a staggered

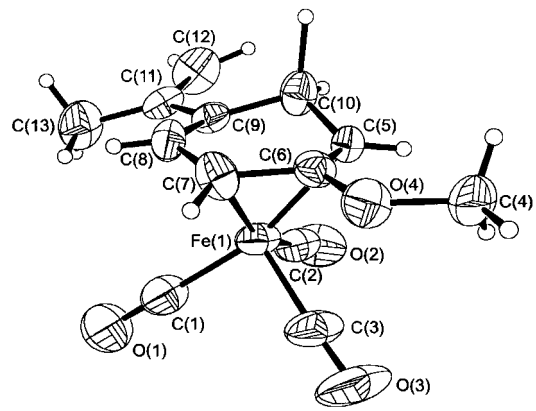

Fig. 3. Ortex plot of cation in **2a**. Ellipsoids represented at the 30% probability level.

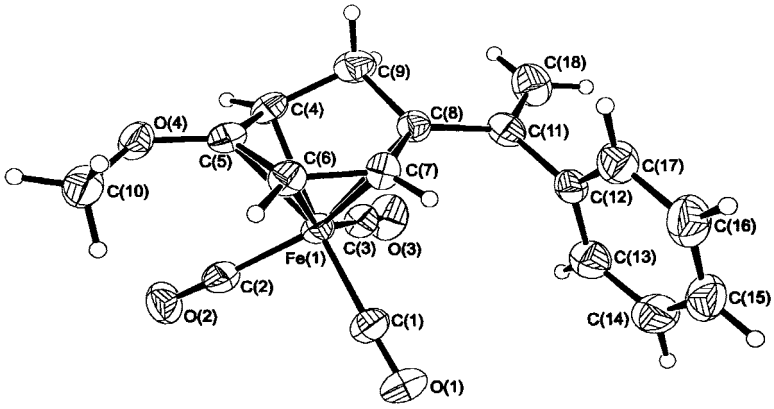

Fig. 4. Ortex plot of cation in **2d**. Ellipsoids represented at the 30% probability level.

conformation so that the pendant alkene does not eclipse any of the three carbonyl vectors in **2a** and **2d** and lies between the two carbonyls of **4b**. The angle between the carbonyls straddling the central methines of the dienyls in **2a** and **2d** (C(1)–Fe(1)–C(3) = 91.9° and C(1)–Fe(1)–C(32) = 92.6°) is compressed with respect to the other angles in the $Fe(CO_3)$ groups (95.9–96.5°). All the structures show that the η^5-portions of the cyclohexadienyl systems are completely flat and they lie in an almost coplanar (**2a** is more distorted) pseudo-*trans* arrangement with respect to the alkenes which are inclined away from the metal-bound face of the working ligand (dihedral angles: **2a** C(8)–C(9)–C(11)–C(12) = 161.5(7); **2d** C(7)–C(8)–C(11)–C(18) = 173.2(8); **4b** C(24)–C(25)–C(28)–C(29) = 170.1(7)°). The bond lengths of the alkenes do not differ significantly from one another (**2a** C(11)–C(12) = 1.356(11); **2d** C(11)–C(18) = 1.346(11); **4b** C(28)–C(29) = 1.297(9) Å) or from the 'normal' sp^2–sp^2 double bond length (1.32 Å) [16]. The single bond which appends the alkenes to the dienyl system is also not significantly different between these examples (**2a** C(9)–C(11) = 1.486(9); **2d** C(8)–C(11) = 1.484(10); **4b** C(25)–C(28) = 1.464(10) Å) or from a normal sp^2–sp^2 single bond (1.48 Å) [16]. In all cases, the iron atoms do not lie directly below the centroids of the unsymmetrical dienyl systems with the iron to alkene-substituted carbon distances (**2a** Fe(1)–C(9) = 2.230(4); **2d** Fe(1)–C(8) = 2.290(7); **4b** Fe(1)–C(25) = 2.282(6) Å) being significantly longer than the iron to unsubstituted-termini distances of the dienyls (**2a** Fe(1)–C(5) = 2.146(6); **2d** Fe(1)–C(4) = 2.131(7); **4b** Fe(1)–C(21) = 2.155(7) Å). Comparison with the literature reveals that tricarbonyl(1-methyl-4-methoxycyclohexadienyl)iron(1 +) [17] exhibits a similar distortion with the 1-methyl-substituted carbon to iron bond being significantly lengthened (2.245(8)) with respect to the far end of the dienyl (adjacent to the methoxy group) to iron bond (2.165(7) Å; Δ 0.080 Å). These differences may be largely due to steric hindrance [17] and indeed compound **2a** has a similar difference in the distances between the iron to dienyl termini (Δ 0.084 Å). This is smaller than **2d** (Δ 0.159 Å) and **4b** (Δ 0.127 Å) due to the added steric bulk of the phenyl groups on the alkene and phosphine, respectively. In the case of tricarbonyl(2-methoxycyclohexadienyl)-iron(1 +) (2.186(8); 2.172(6) Å) [17] the bond lengths of the iron to dienyl termini are only very slightly different (Δ 0.014 Å) and this may not be crystallographically significant. Molecular orbital calculations show that π-donor substituents induce a subtle slipping of the metal away from the far terminal carbon, partially decomplexing it and causing it to become more electrophillic. The well-known *para*-directing ability of the 2-methoxy substituent is related to this subtle distortion and it has been noted that small distortions within a molecule may have large consequences on its

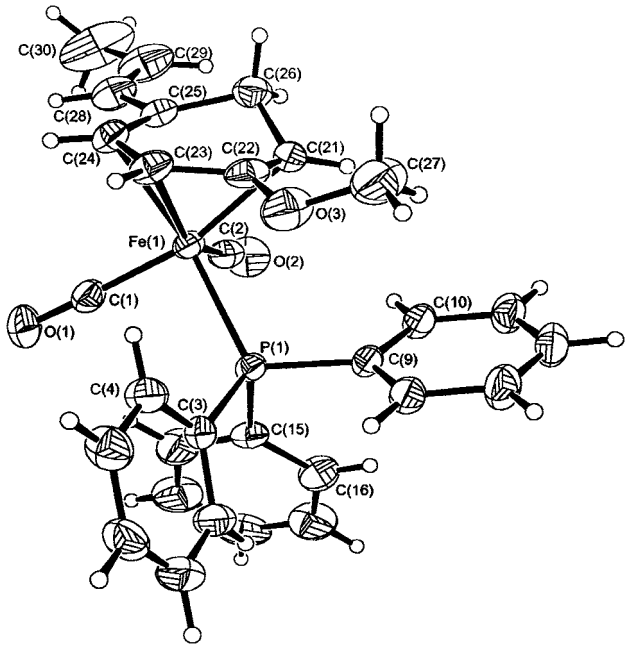

Fig. 5. Ortex plot of cation in **4b**. Ellipsoids represented at the 30% probability level.

Table 1
Selected bond lengths and angles for structures **2a**, **2d** and **4b**

Portion of Structure	**2a**		**2d**		**4b**	
	Atoms	Length (Å) or angle (°)	Atoms	Length (Å) or angle (°)	Atoms	Length (Å) or angle (°)
Pendant Alkene	C(9)–C(11)	1.486(9)	C(8)–C(11)	1.484(10)	C(25)–C(28)	1.464(10)
	C(12)–C(11)	1.356(11)	C(11)–C(18)	1.346(11)	C(28)–C(29)	1.297(9)
	C(11)–C(13)	1.460(11)	C(11)–C(12)	1.486(11)	C(29)–C(30)	1.511(17)
	C(9)–C(11)–C(12)	120.7	C(8)–C(11)–C(18)	120.8	C(25)–C(28)–C(29)	125.5
Iron to diene	Fe(1)–C(9)	2.230(4)	Fe(1)–C(8)	2.290(7)	Fe(1)–C(25)	2.282(6)
	Fe(1)–C(8)	2.216(6)	Fe(1)–C(7)	2.107(8)	Fe(1)–C(24)	2.133(6)
	Fe(1)–C(7)	2.091(7)	Fe(1)–C(6)	2.097(7)	Fe(1)–C(23)	2.108(6)
	Fe(1)–C(6)	2.198(6)	Fe(1)–C(5)	2.205(7)	Fe(1)–C(22)	2.179(6)
	Fe(1)–C(5)	2.146(6)	Fe(1)–C(4)	2.131(7)	Fe(1)–C(21)	2.155(7)
	C(5)–Fe(1)–C(9)	66.5	C(4)–Fe(1)–C(8)	64.7	C(21)–Fe(1)–C(25)	64.9
Auxiliary ligands	Fe(1)–C(1)	1.803(9)	Fe(1)–C(1)	1.830(8)	Fe(1)–C(1)	1.781(6)
	Fe(1)–C(2)	1.819(9)	Fe(1)–C(2)	1.821(9)	Fe(1)–C(2)	1.779(7)
	Fe(1)–C(3)	1.808(9)	Fe(1)–C(3)	1.836(10)		
					Fe(1)–P(1)	2.264(3)
	C(1)–O(1)	1.127(11)	C(1)–O(1)	1.121(9)	C(1)–O(1)	1.129(6)
	C(2)–O(2)	1.125(11)	C(2)–O(2)	1.109(9)	C(2)–O(2)	1.139(7)
	C(3)–O(3)	1.127(11)	C(3)–O(3)	1.128(9)		
	C(1)–Fe(1)–C(2)	96.5	C(1)–Fe(1)–C(2)	92.6	C(1)–Fe(1)–C(2)	99.9
	C(1)–Fe(1)–C(3)	91.9	C(1)–Fe(1)–C(3)	96.1	C(1)–Fe(1)–P(1)	88.1
	C(2)–Fe(1)–C(3)	96.2	C(2)–Fe(1)–C(3)	95.9	C(1)–Fe(1)–C(2)	91.2
	Fe(1)–C(1)–O(1)	178.4	Fe(1)–C(1)–O(1)	178.5	Fe(1)–C(1)–O(1)	177.7
	Fe(1)–C(2)–O(2)	177.1	Fe(1)–C(2)–O(2)	177.3	Fe(1)–C(2)–O(2)	177.6
	Fe(1)–C(3)–O(3)	177.6	Fe(1)–C(3)–O(3)	178.0		

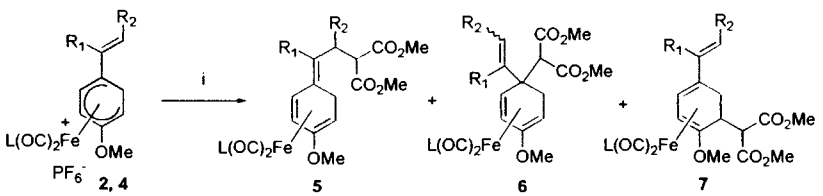

Scheme 2. *Reagents and conditions*: $CH(CO_2Me)_2M$, THF, 0°C.

reactivity [17]. The sizeable distortions evident in structures **2a**, **2d** and **4b** are probably due in large part to steric hindrance between the alkenes and $Fe(CO_2)L$ groups but a small amount of π-orbital overlap from the vinyl group may also contribute and cannot be ruled out since the alkenes all have a similar preferred orientation. This may in turn facilitate directed conjugate addition to the far end of the alkene (see Section 2.3).

2.3. Nucleophile additions to *2* and *4*

The regiochemistry of nucleophillic addition to these alkenyl-extended cyclohexadienyl salts is of paramount importance if these complexes are to be used in synthesis and so investigation of the mode of attack of various types of nucleophiles must be addressed. Cuprates are known to add in a conjugate sense to α,β-unsaturated ketones or esters and this has been established for these complexes with diasteroselectivities as high as 1:8 and reported elsewhere [18]. Stabilised enolates are often used as building blocks in synthesis and can add in a variety of modes, so we chose to examine the regiochemical outcome of dimethyl malonate addition to **2** and **4**. Compounds **5**–**7** (Scheme 2) are all possible products from these reactions and their distributions are presented in Table 2. (The overall isolated yields for these transformations were low (30–40%) but the ratio of products was deduced from the NMR of the crude material after workup and so is expected to reflect the

Table 2
Results for the addition of the sodium and lithium enolates of dimethyl malonate to **2** and **4**

Entry	R_1	R_2	L	M	Ratio (compound)		
					5	**6**	**7**
1	Me	H	CO	Na	<1 (**5a**)	>99 (**6a**)	<1
2	H	Me	CO	Na	<1 (**5b**)	>99 (**6b**)	<1
3 [a]	Me	Me	CO	Na	<1 (**5c**)	>99 (**6c**)	<1
4	Ph	H	CO	Na	65 (**5d**)	35 (**6d**)	<1
5	Me	H	CO	Li	70 (**5a**)	30 (**6a**)	<1
6	H	Me	CO	Li	25 (2:3) [b] (**5b**)	75 (**6b**)	<1
7 [a]	Me	Me	CO	Li	20 (2:3) [b](**5c**)	80 (**6c**)	<1
8	Ph	H	CO	Li	>99 (**5d**)	<1 (**6d**)	<1
9	Me	H	PPh_3	Li/Na	>99 (**5aPPh_3**)	<1 (**6aPPh_3**)	<1
10	H	Me	PPh_3	Li/Na	>99 (1:3) [b] (**5bPPh_3**)	<1 (**6bPPh_3**)	<1
11	Ph	H	PPh_3	Li/Na	>99 (**5dPPh_3**)	<1 (**6dPPh_3**)	<1

[a] *E*/*Z* stereochemistry could not be unambiguously assigned for the 2-butenyl salts.
[b] Ratio of diastereoisomers at the β-position was determined by ^{1}H-NMR.

true product distribution.) Compound **7** (cf. Fig. 2d, 1-addition), was not observed due to the methoxy substituent at C2. Products **5** and **6** (cf. Fig. 2d, 2′- and 3-addition, respectively) were obtained and the ratio of their distributions was found to be dependent on the nature of the malonyl counterion and the ligand set at iron. Addition of sodium enolates to **2** afforded the 3-addition (cf. Fig. 2d) products **6** (Table 2, entries 1–4), but on addition of lithium enolates there was a tendency to form significant amounts of the 2′-adducts, **5** (Table 2, entries 5–8). Ligand exchange to form the triphenylphosphine salts **4** followed by addition of either the sodium or lithium enolates afforded exclusively the 2′-adducts, **5**. Therefore, almost total 3- or 2′-regiocontrol may be obtained by the judicious choice of metal counterion (dependant on its coordinating ability) and ligand set (dependant on its size). (Note that in entry 4, Table 2, incomplete control arises here for steric reasons.)

Three stereochemical issues arise from the formation of **5** or **6**. In the first case, e.g. **5**, either configuration of the exocyclic triene could be formed and it was established by n.O.e. experiments that only a single alkene was observed, assigned as the *E* configuration (Scheme 2). Since equilibration of the alkene after nucleophilic addition is unlikely, as the presence of an α-methyl or phenyl substituent (**5a**,**c**,**d** and **5aPPh_3**, **cPPh_3**) reduces the likelihood of total selective interconversion of the exocyclic trienes, we favour the explanation based on kinetic control during approach of the nucleophiles. This suggests that the orientation adopted in the solid state for each cationic complex (Figs. 3–5) is probably the reacting conformer. The further stereochemical consequence of the conjugate addition pathway occurs if the vinyl terminus is substituted in some way, introducing a prochiral group, which may undergo attack from either face (cf. Fig. 2b, $R_2 \neq H$). Compounds **2b**,**c** and **4b** address this issue and malonate additions to these salts afforded diastereomeric mixtures in the ratio 2:3 for the products **5b** and **5c** and 1:3 for **5bPPh_3** reflecting the greater steric bulk of the phosphine ligand leading to a higher degree of facial selectivity. Notably, the ratio of diasteroeisomers is independent of the counterion used in the malonate enolate. The third stereochemical issue arises during the formation of the products **6** (cf. Fig. 2d, 3-addition) which were all expected to exhibit *trans* addition of the malonyl group by analogy with overwhelming literature precedence. An X-ray diffraction study of **6a** and an Ortex [15] diagram of its molecular structure are shown in Fig. 6 together with selected bond lengths and angles (see Table 3 for crystallographic data and structure refinement). Only poorly diffracting crystals could be grown of **6a** and so the structure is not highly refined ($R = 13\%$), however, it can be seen that addition is indeed from the M-exo face. The other structural features of the crystal are unremarkable and are in agreement with the literature precedents for bond lengths and angles within other unsymmetrically substituted η^4-tricarbonyliron complexed dienes [19].

Inspection of complexes **5a**, **c** and **d** reveals that a new prochiral group (cf. Fig. 2c) has been formed adjacent to the working ligand. Exocyclic trienes of this

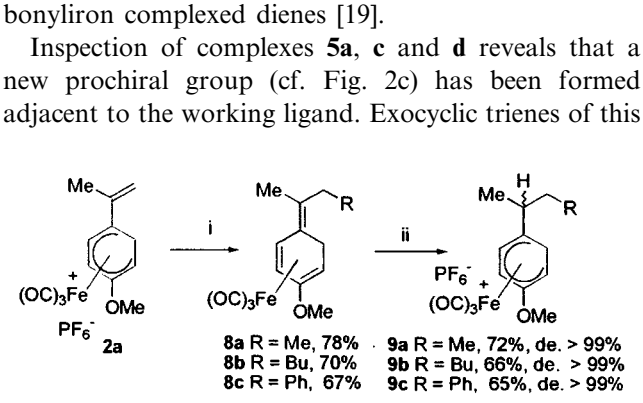

Scheme 3. *Reagents and conditions*: (1) R_2CuLi, THF, −30°C; (2) HPF_6, CH_2Cl_2, 0°C.

type may undergo protonation at the 1′-site leading to reformation of the cationic working ligand and we have investigated the stereochemical outcome of such reactions in the series of trienes, **8**, shown in Scheme 3. Thus, cuprate additions to **2a** proceeded with complete regio- and stereocontrol to afford **8**, which were protonated with HPF_6 to reform the η^5-cyclohexadienyl moiety. Protonation could proceed from either side of the prochiral group leading to a mixture of diasteroeisomers, but inspection of the ^{1}H- and ^{13}C-NMR indicated that only one diastereoisomer had been formed in each case but the relative stereochemistry could not be determined from these data. No crystals could be obtained from any of the products **9** in order resolve this issue and so a second sequence of reactions was designed in which a series of three organoiron-mediated reactions were combined to implement long-range stereocontrol [21] (Scheme 4).

Starting from **10** [20] nucleophile addition as before followed by removal of the OH group formed the cationic product **11** [21]. This was reacted with dimethyl cuprate to afford the single isomer of the exocyclic triene **12** [21] as shown. Salt formation by protonation with HPF_6 reformed the η^5-dienyl system **13** [21] which unfortunately did not provide us with X-ray quality crystals and so this was further elaborated by enolate addition to the far terminus of the dienyl system followed by ligand exchange to form the dicarbonyl triphenylphosphine adduct **15** [21]. This replacement of an auxiliary ligand does not interfere with the stereocenters in the working ligand.[2] The product **15** was crystallised to afford single crystals, which proved suitable for X-ray analysis [21]. The protonation event was clearly seen to have taken place from the M-exo face of the molecule and the relative stereochemistry between C5 and C1′, formed by the long-range chirality relay, was assigned as 5*S*,1′*S*,5*R**,1′*R** [21,22].

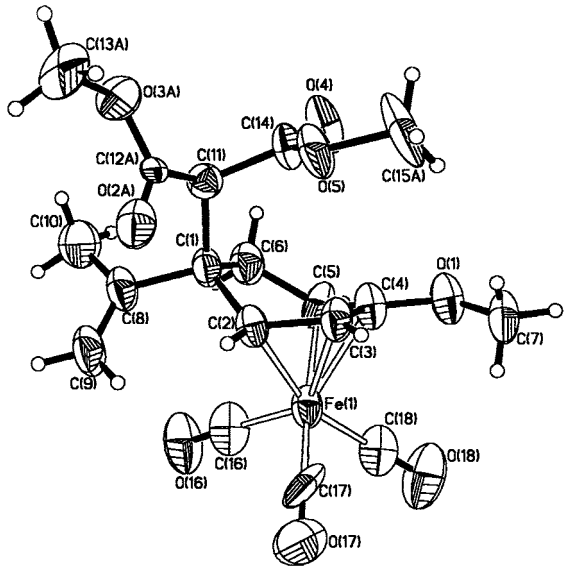

Fig. 6. Ortex diagram of **6a**. Ellipsoids represented at the 50% probability level. For clarity only major components of disorder in the ester groups are shown. Selected bond lengths (Å): C(1)–C(8) = 1.596; C(8)–C(9) = 1.314; C(8)–C(10) = 1.473; C(1)–C(11) = 1.587; Fe(1)–C(2) = 2.104; Fe(1)–C(3) = 2.080; Fe(1)–C(4) = 2.085; Fe(1)–C(5) = 2.117; Fe(1)–C(16) = 1.837; Fe(1)–C(17) = 1.666; Fe(1)–C(18) = 1.781. Selected bond angles (°): C(10)–C(8)–C(1) = 114.4; C(9)–C(8)–C(1) = 123.8; Fe(1)–C(16)–O(16) = 178.0; Fe(1)–C(17)–O(17) = 176.3; Fe(1)–C(18)–O(18) = 175.6.

3. Conclusions

We have shown that judicious choice of nucleophile, counter ion and ligand set, may promote complete regio- and significant stereocontrol in conjugate addition to the remote terminus of alkenyl-extended cyclohexadienyl salts and that the acid-induced reactivation of the emergent exocyclic trienes to reform the η^5-salts is completely stereoselective. The reaction sequence from **11** to **14** is illustrative of these synthetically useful steps and makes use of three organoiron-promoted nucleophile additions during which the combined 1,3/1′,2′ sequence, including the protonation step, creates two chiral centres four atoms apart. The planar chirality of the metal complex controls the formation of both centres and so we have demonstrated in this reaction sequence a long-range relay of chirality via the metal.

4. Experimental

4.1. General methods

All reactions were performed under a nitrogen atmosphere. Diethyl ether and THF were freshly distilled from sodium benzophenone ketyl. The dimethoxy cyclohexadienyl complex **1** was prepared according to the literature procedure [4]. All other chemicals and reagents were used as received without further purification. ^{1}H-NMR spectra were measured on a JEOL EX 270 spectrometer operating at 270 MHz or a Varian Unity 400 spectrometer operating at 400 MHz. ^{13}C-NMR spectra were obtained on a JEOL EX 270 spectrometer operating at 67 MHz. FTIR spectra were obtained on a Perkin–Elmer 1720X as a thin film. Relative peak heights for MS are shown in parentheses.

4.2. General procedure for the formation of salts *2*

Following the work of Seebach and Neuman [23] the required alkenylbromide (two equivalents) was dis-

[2] All the products reported in this paper have been prepared in racemic form and stereoisomers illustrated depict only relative stereochemistry.

Table 3
Crystal data and structure refinement for **2a, 2d, 4b** and **6a**

Compound	**2a**	**2d**	**4b**	**6a**
Empirical formula	$C_{13}H_{13}O_4PF_6Fe$	$C_{18}H_{15}O_4PF_6Fe$	$C_{30}H_{28}O_3P_2F_6Fe$	$C_{17}H_{20}O_8Fe$
Formula weight	449.5	496.12	668.31	408.18
Crystal system	Monoclinic	Orthorhombic	Triclinic	Triclinic
Space group	$P2_1/n$	$P2_12_12_1$	P-1 (no. 2)	P-1
Unit cell dimensions				
a (Å)	14.223(6)	9.415(1)	9.741(3)	10.185(7)
b (Å)	8.087(3)	14.109(2)	10.852(2)	10.436(7)
c (Å)	14.992(5)	15.013(2)	16.153(3)	11.142(7)
α (°)	90	90	87.50(2)	63.49(5)
β (°)	90.82(4)	90	78.90(2)	77.14(5)
γ (°)	90	90	63.37(2)	65.81(5)
U (Å^3)	1716.2	1994.3	1500.1	942.4
Z	4	4	2	2
Temperature (K)	293(2)	293(2)	293(2)	293(2)
$F(000)$	902	1000	742	424
$D_{calc.}$ (mg m^{-3})	1.74	1.65	1.61	1.40
μ(Mo–K$_\alpha$) (mm^{-1})	1.048	0.914	0.677	0.822
Crystal size (mm)	$0.20\times0.25\times0.25$	$0.30\times0.30\times0.30$	$0.30\times0.30\times0.30$	$0.48\times0.41\times0.19$
Diffractometer	CAD4 automatic 4-circle diffractometer	CAD4 automatic 4-circle diffractometer	CAD4 automatic 4-circle diffractometer	Siemens P4
λ(Mo–K$_\alpha$) (Å)	0.71073	0.71073	0.71073	0.71073
Data measured	3030	1826	5017	4050
Unique data	1449	1326	3472	3827
R_{int}	0.0280	0.1315	0.0110	0.0757
Final R indices $[I>2\sigma(I)]$	2680	1798	4703	2306
Parameters/restraints	284/0	281/0	395/0	275/23
wR_2, R_1 (all data)	0.1632, 0.1146	0.1150, 0.0790	0.1239, 0.0675	0.3532, 0.1890
wR_2, R_1 $[I>2\sigma(I)]$	0.1387, 0.0581	0.0977, 0.0415	0.1159, 0.0439	0.3087, 0.1320
S (all data)	1.079	1.062	1.058	1.181
Largest difference peak and hole (e Å^{-3})	0.486 and −0.695	0.362 and −0.327	0.581 and −0.301	2.047 and −1.206

solved in dry diethyl ether and added slowly to a cooled (−78°C) solution of ^{t}BuLi (1.7 M. in hexanes, four equivalents) in dry diethyl ether. The solution was stirred for 1 h and then the temperature of the reaction mixture was reduced to −100°C followed by addition of **1** (or **10** for the formation of **11**) as slurry in dichloromethane via a wide bore cannula. The mixture was allowed to warm to room temperature and was poured into a separating funnel charged with water. Extraction with diethyl ether (three portions), washing with water (three portions) followed by drying ($MgSO_4$) and removal of the solvent in vacuo afforded brown oils in all cases. These were partially purified by flash chromatography through a 3 cm plug of basic alumina in a 5 cm diameter glass sinter funnel with diethyl ether as the eluant to afford orange oils after removal of the solvent. The oils were dissolved in acetic anhydride and cooled to 0°C followed by dropwise addition of hexafluorophosphoric acid (40% in water). The mixtures were poured into diethyl ether and the solid material was collected by filtration. The salts were further purified by reprecipitation from acetone–ether several times to afford the required cationic complexes as air stable yellow solids.

4.2.1. Tricarbonyl[(1,2,3,4,5-η)-1-(1′-methylethenyl)-4-methoxycyclohexadienyl]iron(1+) hexafluorophosphate(1−) ***2a***

Experimental procedures and work up were as described in Section 4.2. Experimental details: 2-bromopropene (3.390 g, 28.0 mmol); **1** (4.670 g, 14.0 mmol). Yield: 4.140 g, 68% based on **1**. Obtained as a pale yellow solid. ^{1}H-NMR (acetone-d_6, 270 MHz): δ 6.84 (dd, 1H, $J=2.6$, 3.6 Hz, C3–H), 5.72 (d, 1H, $J=6.3$ Hz, C2–H), 5.62 (s, 1H, $CH_3C{=}CH_2$), 5.59 (s, 1H, $CH_3C{=}CH_2$), 4.03 (m, 1H, C5–H), 3.84 (s, 3H, OCH_3), 3.41 (dd, 1H, $J=6.6$, 14.5 Hz, C6β–H), 2.20 (bd, 1H, $J=14.5$ Hz, C6α–H), 1.75 (s, 3H, $CH_3C{=}CH_2$). IR (cm^{-1}):ν (CO) 2108, 2067, 2038, 1635. EIMS; m/z: 290 ([M]$^+$, 1.5), 262 ([M$^+$ − CO], 23), 234 ([M$^+$ − 2CO], 12), 206 ([M$^+$ − 3CO], 48), 148 (100), 107 (54). Anal. Found: C, 35.9; H, 2.9. Calc. for $C_{13}H_{13}F_6FeO_4P$: C, 35.9; H, 3.0%. The structure was also established by X-ray analysis (Fig. 3, Tables 1 and 3).

4.2.2. (E)-Tricarbonyl[(1,2,3,4,5-η)-4-methoxy-1-(2′-methylethenyl)cyclohexadienyl]iron(1+) hexafluorophosphate(1−) ***2b***

Experimental procedures and work up were as described in Section 4.2. Experimental details: (*E*/*Z*)-1-

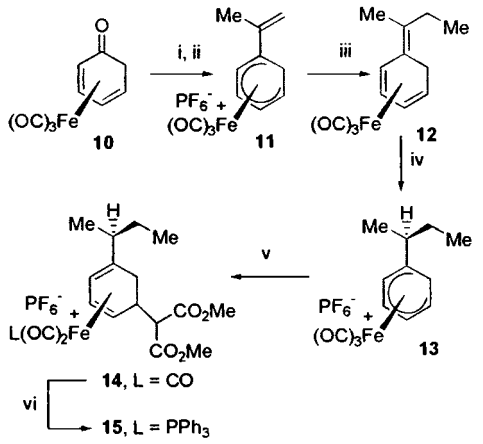

Scheme 4. *Reagents and conditions*: (1) 2-lithiopropene, THF, −100°C; (2) HPF_6, Ac_2O, 0°C; (3) Me_2CuLi, THF, −30°C; (4) HPF_6, Ac_2O, 0°C; (5) $CH(CO_2Me)_2Na$, THF, 0°C; (6) Me_3NO, PPh_3, acetone.

bromopropene (0.660 g, 5.40 mmol); **1** (0.903 g, 2.70 mmol). Yield: 0.694 g, 59% based on **1**. Obtained as a pale yellow solid. ^{1}H-NMR (acetone-d_6, 270 MHz): δ 7.23 (dd, 1H, $J = 2.6$, 5.9 Hz, C3–H), 6.72 (dq, 1H, $J = 7.5$, 15.5 Hz, HC=C*H*CH$_3$), 5.98 (d, 1H, $J = 5.9$ Hz, C2–H), 5.67 (d, 1H, $J = 15.5$ Hz, *H*C=CHCH$_3$), 4.30 (m, 1H, C5–H), 3.99 (s, 3H, OC*H*$_3$), 3.83 (dd, 1H, $J = 6.53$, 15.2 Hz, C6β–H), 2.76 (bd, 1H, $J = 14.5$ Hz, C6α–H), 1.91 (dd, 3H, $J = 1.7$, 7.6 Hz, HC=CHC*H*$_3$). IR (cm^{-1}): ν(CO) 2106, 2043. EIMS; m/z: 290 ([M$^+$ + H], 0.4), 262 ([M$^+$ + H − CO], 8), 233 ([M$^+$ − 2CO], 0.3), 205 ([M$^+$ − 3CO], 2), 178 (16), 121 (61). FABMS; m/z: Mass calc. for $[C_{13}H_{14}FeO_4]^+$: 290.024. Found: 290.024.

4.2.3. (E)-Tricarbonyl[(1,2,3,4,5-η)-4-methoxy-1-(1′,2′-dimethylethenyl)cyclohexadienyl]iron(1 +) hexafluorophosphate(1 −) **2c**

Experimental procedures and work up were as described in Section 4.2. Experimental details: (*E*/*Z*)-2-bromobut-2-ene (0.737 g, 5.40 mmol); **1** (0.901 g, 2.70 mmol). Yield: 0.762 g, 62% based on **1**. Obtained as a pale yellow solid. ^{1}H-NMR (acetone-d_6, 270 MHz): δ 7.26 (dd, 1H, $J = 2.3$, 5.9 Hz, C3–H), 5.96 (m, 2H, C2–H and CH$_3$C=C*H*CH$_3$), 4.27 (m, 1H, C5–H), 4.02 (s, 3H, OC*H*$_3$), 3.62 (dd, 1H, $J = 7.3$, 15.5 Hz, C6β–H), 2.76 (bd, 1H, $J = 15.5$ Hz, C6α–H), 1.96 (s, 3H, C*H*$_3$C=CHCH$_3$), 1.74 (d, 3H, $J = 7.3$ Hz, CH$_3$C=CHC*H*$_3$). IR (cm^{-1}): ν(CO) 2104, 2053, 2038. EIMS; m/z: 304 ([M$^+$ + H], 0.2), 276 ([M$^+$ + H − CO], 3), 248 ([M$^+$ + H − 2CO], 2), 220 ([M$^+$ + H − 3CO], 5), 219 ([M$^+$ − 3CO], 1). CIMS; m/z: Mass calc. for $[C_{14}H_{15}FeO_4]^+$: 304.0398. Found: 304.0398.

4.2.4. Tricarbonyl[(1,2,3,4,5-η)-1-(ethenyl-1′-phenyl)-4-methoxycyclohexadienyl]iron(1 +) hexafluorophosphate(1 −) **2d**

Experimental procedures and work up were as described in Section 4.2. Experimental details: 1-bromostyrene (1.990 g, 10.9 mmol); **1** (1.832 g, 5.50 mmol). Yield: 1.428 g, 52% based on **1**. Obtained as a pale yellow solid. ^{1}H-NMR (acetone-d_6, 400 MHz): δ 7.48 (m, 3H, Ph), 7.25 (m, 2H, Ph), 7.12 (dd, 1H, $J = 2.4$, 6.0 Hz, C3–H), 6.09 (s, 1H, PhC=CH*H*), 5.74 (s, 1H, PhC=C*H*H), 5.65 (d, 1H, $J = 6.0$ Hz, C2–H), 4.44 (m, 1H, C5–H), 3.99 (s, 3H, OC*H*$_3$), 3.74 (dd, 1H, $J = 5.1$, 15.2 Hz, C6β–H), 2.67 (bd, 1H, $J = 15.2$ Hz, C6α–H). IR (cm^{-1}): ν(CO): 2107, 2058, 2035. FABMS; m/z: 351 ([M]$^+$, 100), 323 ([M$^+$ − CO], 16), 295 ([M$^+$ − 2CO], 2), 267 ([M$^+$ − 3CO], 11), 211 (9), 103 (9). FABMS; m/z: Mass calc. for $[C_{18}H_{15}FeO_4]^+$: 351.0320. Found: 351.0322. The structure was also established by X-ray analysis (Fig. 4, Tables 1 and 3).

4.3. General procedure for the formation of dicarbonyltriphenylphosphine derivatives

Following the work of Birch and Kelley [24] the neutral vinyl adducts (one equivalent) formed above as intermediates were dissolved in acetone. Trimethylamine-*N*-oxide (six equivalents) and triphenylphosphine (seven equivalents) were added and the mixtures were heated at reflux for 24 h. After cooling, the solutions were poured into a 1:9 mixture of diethyl ether–petroleum ether (40/60). Most of the excess triphenylphosphine was removed in this way as a fine precipitate and the solutions were concentrated after filtration to afford yellow solids. Purification by column chromatography on silica gel with 1:30:69 triethylamine–diethyl ether–petroleum ether (40/60) as the eluant afforded the required compounds as yellow solids.

4.3.1. Dicarbonyl[2,3,4,5-η)-1,4-dimethoxy-1-(1′-methylethenyl)cyclohexadiene]triphenylphosphineiron(0) **3a**

Experimental procedures and work up were as described in Section 4.3. Experimental details: **1** (1.290 g, 3.55 mmol). Yield: 0.767 g, 39% based on **1**. Obtained as a very pale yellow solid. ^{1}H-NMR (CHCl$_3$-*d*, 270 MHz): δ 7.3–7.7 (m, 15H, Ph), 6.74 (s, 1H, CH$_3$C=CH*H*), 6.65 (s, 1H, CH$_3$C=C*H*H), 4.22 (m, 1H, C3–H), 3.38 (s, 3H, OC*H*$_3$), 3.05 (m, 1H, C5–H), 2.88 (s, 3H, OC*H*$_3$), 1.94 (t, 2H, $J = 3.6$ Hz, C6α–H, C6β–H), 1.88 (m, 1H, C2–H), 1.53 (s, 3H, C*H*$_3$C=CH$_2$). IR (cm^{-1}): ν(CO) 1973, 1911, 1484, 1436, 1311, 1184, 1120. FABMS; m/z: very weak ions, 554 ([M]$^+$), 526 ([M$^+$ − CO]), 498 ([M$^+$ − 2CO]). FABMS; m/z: Mass calc. for $[C_{30}H_{28}FeO_3P]^+$: 523.1125. Found: 523.1125.

4.3.2. (E/Z)-Dicarbonyl[2,3,4,5-η)-1,4-dimethoxy-1-(2′-methylethenyl)cyclohexadiene]triphenylphosphineiron(0) ***3b***

Experimental procedures and work up were as described in Section 4.3. Experimental details: **1** (5.00 g, 14.0 mmol). Yield: 2.482 g, 32% based on **1**. Obtained as a very pale yellow solid. ^{1}H-NMR ($CHCl_3$-*d*, 270 MHz): δ 7.3–7.7 (m, 15H, Ph), 5.30 (dq, 1H, $J = 7.3$, 11.6 Hz, HC=C*H*CH_3), 4.99 (dq, 1H, $J = 1.7$, 11.6 Hz, *H*C=CHCH_3), 3.86 (m, 1H, C3–H), 3.35 (s, 3H, OCH_3), 3.09 (m, 4H, OCH_3 and C5–H), 2.17 (dt, 1H, $J = 3.6$, 14.5 Hz, C6β–H), 2.07 (t, 1H, $J = 7.3$ Hz, C2–H), 1.89 (ddd, 1H, $J = 2.3$, 4.6, 14.5 Hz, C6α–H), 1.62 (dt, 3H, 1.7, 7.3 Hz, HC=CHC*H*$_3$). IR (cm^{-1}): *ν*(CO): 1973, 1911, 1482, 1434, 1219, 1091, 1073, 1028. EIMS; *m*/*z*: 264 ([$M^+ - CO - PPh_3$], 2), 262 (PPh_3, 100), 205 ([$M^+ - CO - PPh_3 - OCH_3$], 1), 183 (48), 181 ([$M^+ - 2CO - PPh_3 + H$], 2), 148 (73), 133 (18), 121 (35).

4.3.3. (E/Z)-Dicarbonyl[2,3,4,5-η)-1,4-dimethoxy-1-(1′,2′-dimethylethenyl)cyclohexadiene]triphenylphosphineiron(0) ***3c***

Experimental procedures and work up were as described in Section 4.3. Experimental details: **1** (5.00 g, 14.0 mmol). Yield: 1.164 g, 16% based on **1**. Obtained as a very pale yellow solid as a mixture of two inseparable configurational isomers in the ratio 1:4, A:B; by NMR. ^{1}H-NMR ($CHCl_3$-*d*, 270 MHz). Configurational isomer A: δ 6.8–7.8 (m, 15H, Ph), 5.46 (1H, q, $J = 6.6$ Hz, CH_3C=C*H*CH_3), 4.26 (ddd, 1H, $J = 2.3$, 7.0, 7.3 Hz, C3–H), 3.18 (m, 1H, C5–H), 3.14 (s, 3H, OCH_3), 2.98 (s, 3H, OCH_3), 2.28 (dd, 1H, $J = 6.9$, 7.0 Hz, C2–H), 2.00–2.20 (m, 2H, C6α–H, C6β–H), 1.52 (s, 3H, CH_3C=CHC*H*$_3$), 1.40 (d, 3H, $J = 6.6$ Hz, C*H*$_3$C=C*H*CH_3). Configurational isomer B: δ 6.8–7.8 (m, 15H, Ph), 5.21 (1H, q, $J = 7.3$ Hz, CH_3C=C*H*CH_3), 3.95 (ddd, 1H, $J = 2.3$, 7.0, 7.3 Hz, C3–H), 3.29 (m, 1H, C5–H), 3.15 (s, 3H, OCH_3), 3.07 (s, 3H, OCH_3), 2.28 (dd, 1H, $J = 6.9$, 7.0 Hz, C2–H), 2.00–2.20 (m, 2H, C6α–H, C6β–H), 1.77 (d, 3H, $J = 7.3$ Hz, CH_3C=CHC*H*$_3$), 1.48 (s, 3H, CH_3C=CHC*H*$_3$). IR (cm^{-1}): *ν*(CO) 1984, 1926, 1485, 1435, 1272, 1093, 1029, 744, 697. FABMS; *m*/*z*: 568 ([M]$^+$, 16), 537 ([$M^+ - OCH_3$], 24), 509 ([$M^+ - OCH_3 - CO$], 10), 481 ([$M^+ - OCH_3 - 2CO$], 45), 480 (100), 349 (51), 318 (91), 263 (PPh_3 + H, 30), 239 (39), 183 (41).

4.3.4. Dicarbonyl[2,3,4,5-η)-1,4-dimethoxy-1-(1′-phenylethenyl)cyclohexadiene]triphenylphosphineiron(0) ***3d***

Experimental procedures and work up were as described in Section 4.3. Experimental details: **1** (1.00 g, 2.70 mmol). Yield: 0.965 g, 58% based on **1**. Obtained as a very pale yellow solid. ^{1}H-NMR (270 MHz, $CHCl_3$-*d*): δ 7.0–7.8 (m, 20H, Ph), 5.17 (s, 2H, PhC=C*H*$_2$), 4.32 (ddd, 1H, $J = 2.3$, 6.3, 6.6 Hz, C3-H), 3.10 (bs, 4H, C5–H and OCH_3), 3.05 (s, 3H, OCH_3), 2.34 (dt, 1H, $J = 3.6$, 14.8 Hz, C6β–H), 2.16 (ddd, 1H, $J = 2.3$, 4.6, 14.8 Hz, C6α–H), 2.03 (dd, 1H, $J = 6.3$, 6.3 Hz, C2–H). IR(cm^{-1}): *ν*(CO) 1974, 1914, 1622, 1435, 1221, 1090. FABMS; *m*/*z*: 616 ([M]$^+$, 22), 560 ([$M^+ - 2CO$], 3), 528 ([$M^+ - 2CO - OCH_3 - H$], ([$M^+ - 2CO - OCH_3 - H$], 100), 349 (31), 318 (46), 298 ([$M^+ - 2CO - PPh_3$], 3), 263 (16), 239 (11), 183 (20). FABMS; *m*/*z*: Mass calc. for [$C_{33}H_{29}FeOP$]$^+$, ($M^+ - 2CO - OCH_3 - H$): 528.1305. Found: 528.1276.

4.4. General procedure for the formation of salts ***4***

Compounds **3** (one equivalent) were dissolved in acetic anhydride (10 ml) and cooled (°C). Excess hexafluorophosphoric acid was added dropwise and the mixtures were stirred for 10 min. The solutions were poured into dry diethyl ether (50 ml) and the yellow precipitates were collected by filtration. These were further purified by reprecipitation from acetone–diethyl ether to afford the required compounds as orange solids.

4.4.1. Dicarbonyl[(1,2,3,4,5-η)-1-(1′-methylethenyl)-4-methoxycyclohexadienyl]triphenylphosphineiron(1 +) hexafluorophosphate(1 −) ***4a***

Experimental procedures and work up were as described in Section 4.4. Experimental details: **3a** (0.615 g, 1.11 mmol). Yield: 0.475 g, 64%. Obtained as an orange solid. ^{1}H-NMR (acetone-d_6, 270 MHz): δ 7.60 (m, 15H, Ph), 7.03 (bs, 1H, C3–H), 5.72 (bs, 1H, C2–H), 5.62 (s, 1H, CH_3C=C*H*H), 5.55 (s, 1H, CH_3C=CH*H*), 3.96 (bs, 1H, C5–H), 2.80 (s, 3H, OCH_3), 2.33 (d, 1H, $J = 14.4$ Hz, C6β–H), 2.05 (m, 1H, C6α–H), 1.86 (s, 3H, C*H*$_3$C=CH$_2$). IR (cm^{-1}): *ν*(CO) 2020, 1985, 1562, 1380, 1264, 1093. FABMS; *m*/*z*: 523 ([M]$^+$, 100), 495 ([$M^+ - CO$], 26), 467 ([$M^+ - 2CO$], 15), 335 (10), 318 (12), 263 (12), 139 (11), 183 (13). FABMS; *m*/*z*: Mass calc. for [$C_{30}H_{28}FeO_3P$]$^+$: 523.1123. Found: 523.1123.

4.4.2. (E)-Dicarbonyl[(1,2,3,4,5-η)-1-(2′-methylethenyl)-4-methoxycyclohexadienyl]triphenylphosphineiron(1 +) hexafluorophosphate(1 −) ***4b***

Experimental procedures and work up were as described in Section 4.4. Experimental details: **3b** (1.300 g, 2.34 mmol). Yield: 1.189 g, 76%. Obtained as an orange solid. ^{1}H-NMR (acetone-d_6, 270 MHz,): δ 7.60 (m, 15H, Ph), 6.65 (bs, 1H, C3–H), 6.34 (dq, 1H, $J = 6.9$, 15.8 Hz, HC=C*H*CH_3), 5.18 (bs, 1H, C2–H), 3.98 (bs, 1H, C5–H), 3.49 (d, 1H, $J = 15.8$ Hz, *H*C=CHCH_3), 2.93 (s, 3H, OCH_3), 2.23 (dd, 1H, $J = 5.6$, 14.4 Hz, C6β–H), 1.70 (m, 1H, C6α–H), 1.77 (d, 3H, $J = 6.9$ Hz, HC=CHC*H*$_3$). IR (cm^{-1}): *ν*(CO) 2032, 1984, 1495, 1464, 1434, 1377, 1239, 1044, 984, 835. Anal. Found: C, 54.1; H, 4.2. Calc. for $C_{30}H_{28}F_6FeO_3P_2$: C, 53.9; H, 4.2%. The structure was also established by X-ray analysis (Fig. 5, Tables 1 and 3).

4.4.3. (E)-Dicarbonyl[(1,2,3,4,5-η)-1-(1′,2′-dimethylethenyl)-4-methoxycyclohexadienyl]triphenylphosphineiron(1 +) hexafluorophosphate(1 −) **4c**

Experimental procedures and work up were as described in Section 4.4. Experimental details: **3c** (1.100 g, 1.90 mmol). Yield: 1.088 g, 84%. Obtained as an orange solid. ^{1}H-NMR (acetone-d_6, 270 MHz): δ 7.3–7.7 (m, 15H, Ph), 7.00 (bs, 1H, C3–H), 6.14 (q, 1H, $J = 6.8$ Hz, $CH_3C{=}CHCH_3$), 5.50 (bm, 1H, C2–H), 3.34 (s, 3H, OCH_3), 3.30 (bm, 1H, C5–H), 2.20 (bd, 1H, 14.5 Hz, C6β–H), 1.75 (d, 3H, $J = 6.8$ Hz, $CH_3C{=}CHCH_3$), 1.70 (bm, 1H, C6α–H), 1.62 (s, 3H, $CH_3C{=}CHCH_3$). IR (cm^{-1}): ν(CO) 2037, 1993, 1489, 1435, 1422, 1094, 896, 846. FABMS; m/z: 537 ([M]$^+$, 100), 509 ([M$^+$ − CO], 56), 481 ([M$^+$ − 2CO], 19), 479 (41), 318 (46), 263 (37), 239 (29), 183 (37). FABMS; m/z: Mass calc. for $[C_{31}H_{30}FeO_3P]^+$: 537.1282. Found: 537.1267.

4.4.4. Dicarbonyl[(1,2,3,4,5-η)-1-(1′-phenylethenyl)-4-methoxycyclohexadienyl]triphenylphosphineiron(1 +) hexafluorophosphate(1 −) **4d**

Experimental procedures and work up were as described in Section 4.4. Experimental details: **3d** (0.974 g, 1.58 mmol). Yield: 0.923 g, 80%. Obtained as an orange solid. ^{1}H-NMR (acetone-d_6, 400 MHz): δ 7.2–7.6 (m, 20H, Ph), 6.98 (bs, 1H, C3–H), 6.95 (s, 1H, PhC=CHH), 5.46 (s, 1H, PhC=CHH), 5.28 (bs, 1H, C2–H), 3.64 (dd, 1H, $J = 5.6$, 14.6 Hz, C6β–H), 3.59 (bs, 1H, C5–H), 2.96 (s, 3H, OCH_3), 2.45 (d, 1H, $J = 14.6$ Hz, C6α–H). IR (cm^{-1}): ν(CO) 2042, 2001, 1495, 1487, 1434, 1378, 1311, 1237, 1093. FABMS; m/z: 585 ([M]$^+$, 100), 557 ([M$^+$ − CO], 16), 529 ([M$^+$ − 2CO], 16), 335 (5), 318 (7), 263 (8), 183 (7). FABMS; m/z: Mass calc. for $[C_{35}H_{30}FeO_3P]^+$: 585.1282. Found: 585.1261.

4.5. General procedure for the addition of dialkyl malonates to **2** and **4**

The dialkyl malonate (two equivalents) was dissolved in dry THF (30 ml) and cooled to −78°C under nitrogen. The appropriate base (lithium bis(trimethylsilyl)amide or NaH) was added (2.1 equivalents) and the mixture was stirred for 30 min. The salts **2** and **4** were added as solids in one portion and the mixture was stirred at −78°C for a further 30 min before being allowed to warm to room temperature. The solution was poured into a separating funnel charged with water and extracted with diethyl ether (three portions). The extracts were combined, washed (three portions of water) and dried over $MgSO_4$ followed by removal of the solvent in vacuo. The residues were purified by column chromatography on silica gel with 20:80; diethyl ether–petroleum ether (40/60) as the eluant to afford the required compounds as yellow solids. Isolated yields are quoted.

4.5.1. (E)-Tricarbonyl[methyl (2,3,4,5-η)-2′-carbomethoxy-4-(4-methoxycyclohexadien-1-ylidene)-pentanoate]iron(0) **5a**

Experimental procedures and work up were as described in Section 4.5. Experimental details: lithium bis(trimethylsilyl)amide (1.5 ml, 1 M in THF, 1.5 mmol). Dimethyl malonate (0.184 g, 1.4 mmol); **2a** (0.300 g, 0.69 mmol). Yield: 0.061 g, 21% based on **2a**. Obtained as a yellow oil. ^{1}H-NMR ($CHCl_3$-d 270 MHz): δ 5.11 (dd, 1H, $J = 2.6$, 6.6 Hz, C3–H), 3.71 (s, 3H, OCH_3), 3.69 (s, 3H, OCH_3), 3.65 (s, 3H, OCH_3), 3.40–3.54 (m, 2H, COCHCO and C5–H), 3.32 (d, 1H, $J = 6.9$ Hz, C2–H), 2.55 (dd, 1H, $J = 8.3$, 13.9 Hz, $CH_3C{=}CHH$), 2.36 (dd, 1H, $J = 7.3$, 14.2 Hz, $CH_3C{=}CH$H), 2.53 (db, 1H, $J = 16.7$ Hz, C6β–H), 2.29 (bd, 1H, $J = 16.7$ Hz, C6α–H), 1.64 (t, 3H, 1.3 Hz, $CH_3C{=}CH_2$). IR (cm^{-1}): ν(CO) 2039, 1962. EIMS; m/z: 420 ([M]$^+$, 3), 364 ([M$^+$ − 2CO], 20), 337 (19), 336 ([M$^+$ − 3CO], 100), 321 (13), 236 (28), 221 (17), 218 (19), 204 (57), 164 (16), 148 (97), 133 (31). EIMS; m/z: Mass calc. for $[C_{17}H_{20}FeO_7]^+$: 392.058. Found: 392.058.

4.5.2. (E)-Tricarbonyl[methyl (2,3,4,5-η)-2′-carbomethoxy-4-(4-methoxycyclohexadien-1-ylidene)-3′-methylbutanoate]iron(0) **5b**

Experimental procedures and work up were as described in Section 4.5. Experimental details: lithium bis(trimethylsilyl)amide (1.5 ml, 1 M in THF, 1.5 mmol). Dimethyl malonate (0.184 g, 1.4 mmol); **2b** (0.300 g, 0.69 mmol). Yield: 0.029 g, 10% based on **2b**. Obtained as yellow oil as a mixture of two inseparable diastereoisomers in the ratio 2:3, A:B; by NMR. ^{1}H-NMR ($CHCl_3$-d, 270 MHz). Diastereoisomer A: δ 5.08 (dd, 1H, $J = 2.3$, 6.6 Hz, C3–H), 5.05 (d, 1H, $J = 11.0$ Hz, C=CHCH), 3.69 (s, 3H, OCH_3), 3.67 (s, 3H, OCH_3), 3.62 (s, 3H, OCH_3), 3.49 (m, 1H, C5–H), 3.19 (d, 1H, $J = 9.2$ Hz, COCHCO), 3.08 (d, 1H, $J = 6.6$ Hz, C2–H), 2.85 (m, 1H, CHCHCH$_3$), 2.60 (m, 1H, C6β–H), 2.25 (m, 1H, C6α–H), 0.90 (d, 3H, $J = 6.3$ Hz, CHCHCH_3). Diastereoisomer B: δ 5.08 (dd, 1H, $J =$ 2.3, 6.6 Hz, C3–H), 5.05 (d, 1H, $J = 11.0$ Hz, C=CHCH), 3.69 (s, 3H, OCH_3), 3.67 (s, 3H, OCH_3), 3.62 (s, 3H, OCH_3), 3.49 (m, 1H, C5–H), 3.17 (d, 1H, $J = 9.2$ Hz, COCHCO), 3.08 (d, 1H, $J = 6.6$ Hz, C2–H), 2.85 (m, 1H, CHCHCH$_3$), 2.60 (m, 1H, C6β–H), 2.25 (m, 1H, C6α–H), 0.90 (d, 3H, $J = 6.3$ Hz, CHCHCH_3). IR (cm^{-1}): ν(CO) 2048, 1986, 1794, 1729, 1562, 1382. EIMS; m/z: 392 ([M$^+$ − CO], 1), 364 ([M$^+$ − 2CO], 1), 336 ([M$^+$ − 3CO], 4), 204 (10), 148 (100), 133 (52), 84 (21), 49(19). EIMS; m/z: Mass calc. for $[C_{17}H_{20}FeO_7]^+$: 392.058. Found: 392.058.

4.5.3. (E)-Tricarbonyl[methyl (2,3,4,5-η)-2-carbomethoxy-4-(4-methoxycyclohexadien-1-ylidene)-3-methylpentanoate]iron(0) ***5c***

Experimental procedures and work up were as described in Section 4.5. Experimental details: lithium bis(trimethylsilyl)amide (1.5 ml, 1 M in THF, 1.5 mmol). Dimethyl malonate (0.184 g, 1.4 mmol); **2c** (0.300 g, 0.67 mmol). Yield: 0.022 g, 8% based on **2c**. Obtained as yellow oil as a mixture of two inseparable diastereoisomers in the ratio 2:3, A:B; by NMR. ^{1}H-NMR ($CHCl_3$-*d*, 270 MHz). Diastereoisomer A: δ 5.15 (dd, 1H, $J = 2.6$, 6.9 Hz, C3–H), 3.75 (s, 3H, OCH_3), 3.74 (s, 3H, OCH_3), 3.67 (s, 3H, OCH_3), 3.47 (dt, 1H, $J = 2.3$, 3.9 Hz, C5–H), 3.40 (d, 1H, $J = 10.9$ Hz, COC*H*CO), 3.30 (d, 1H, $J = 6.9$ Hz, C2–H), 3.10 (dq, 1H, $J = 6.9$, 11.2 Hz, CH_3CCHCH_3), 2.68 (m, 1H, C6β–H), 2.42 (m, 1H, C6α–H), 1.58 (s, 3H, CH_3CHCH_3), 0.97 (d, 3H, $J = 6.9$ Hz, $CH_3CHCHCH_3$). Diastereoisomer B: δ 5.11 (dd, 1H, $J = 2.6$, 6.9 Hz, C3–H), 3.72 (s, 3H, OCH_3), 3.66 (s, 3H, OCH_3), 3.65 (s, 3H, OCH_3), 3.54 (dt, 1H, $J = 2.3$, 3.9 Hz, C5–H), 3.41 (d, 1H, $J = 11.2$ Hz, COC*H*CO), 3.30 (d, 1H, $J = 6.9$ Hz, C2–H), 3.10 (dq, 1H, $J = 6.9$, 11.2 Hz, CH_3CCHCH_3), 2.68 (m, 1H, C6β–H), 2.42 (m, 1H, C6α–H), 1.58 (s, 3H, CH_3CHCH_3), 0.89 (d, 3H, $J = 6.9$ Hz, $CH_3CHCHCH_3$). IR (cm^{-1}): *ν*(CO) 2042, 1968, 1759, 1738, 1489, 1435, 1226, 1173, 1039. EIMS; *m*/*z*: 434 ($[M]^+$, 0.3), 378 ($[M^+ - 2CO]$, 1), 350 ($[M^+ - 3CO]$, 28), 218 (25), 162 (100), 147 (58). EIMS; *m*/*z*: Mass calc. for $[C_{19}H_{22}FeO_8]^+$: 434.0664. Found: 434.0664.

4.5.4. (Z)-Tricarbonyl[methyl (2,3,4,5-η)-2-carboethoxy-4-(4-methoxycyclohexadien-1-ylidene)-4-phenylbutanoate]iron(0) ***5d***

Experimental procedures and work up were as described in Section 4.5. Experimental details: lithium bis(trimethylsilyl)amide (0.85 ml, 1 M in THF, 0.85 mmol). Diethyl malonate (0.128 g, 0.8 mmol); **2d** (0.200 g, 0.40 mmol). Yield: 0.059 g, 29% based on **2d**. ^{1}H-NMR ($CHCl_3$-*d*, 400 MHz): δ 7.35 (m, 3H, Ph), 7.10 (m, 2H, Ph), 5.01 (dd, 1H, $J = 2.4$, 6.8 Hz, C3–H), 4.06 (q, 4H, $J = 7.2$ Hz, $2 \times CH_3CH_2O$), 3.62 (s, 3H, OCH_3), 3.55 (m, 1H, C5–H), 3.13 (d, 1H, $J = 6.8$ Hz, C2–H), 3.10 (dd, 1H, $J = 7.3$, 7.8 Hz, COC*H*CO), 2.84 (dd, 1H, 7.8, 14.4 Hz, PhCC*H*HCH), 2.73 (dd, 1H, 7.8, 14.4 Hz, PhCCH*H*CH), 2.72 (d, 1H, $J = 17.8$ Hz, C6β–H), 2.46 (dd, 1H, $J = 2.0$, 17.8 Hz, C6α–H), 1.19 (t, 6H, $J = 7.2$ Hz, $2 \times CH_3CH_2O$). EIMS; *m*/*z*: Mass calc. for $[C_{25}H_{26}FeO_8]^+$: 510.0977. Found: 510.0977.

4.5.5. (E)-Dicarbonyl[methyl(2,3,4,5-η)-2-carbomethoxy-4-(4-methoxycyclohexadien-1-ylidene)-pentanoate]triphenylphosphineiron(0) ***5aPPh$_3$***

Experimental procedures and work up were as described in Section 4.5. Experimental details: lithium bis(trimethylsilyl)amide (0.85 ml, 1 M in THF, 0.85 mmol). Dimethyl malonate (0.106 g, 0.8 mmol); **4a** (0.250 g, 0.37 mmol). Yield: 0.189 g, 78% based on **4a**. ^{1}H-NMR ($CHCl_3$-*d*, 270 MHz): δ 6.8–7.8 (m, 15H, Ph), 3.98 (ddd, 1H, $J = 2.5$, 4.6, 6.9 Hz, C3–H), 3.71 (dd, 1H, $J = 6.6$, 9.2 Hz, COC*H*CO), 3.51 (s, 3H, OCH_3), 3.40 (m, 1H, C5–H), 3.29 (s, 3H, OCH_3), 3.14 (s, 3H, OCH_3), 2.90 (dd, 1H, $J = 9.2$, 14.2 Hz, $CH_3CCHHCH$), 2.86 (bd, 1H, $J = 17.5$ Hz, C6β–H), 2.64 (dd, 1H, $J = 6.9$, 7.6 Hz, C2–H), 2.56 (dd, 1H, $J = 6.6$, 14.2 Hz, $CH_3CCHHCH$), 2.34 (dd, 1H, $J = 5.6$, 17.5 Hz, C6α–H), 1.58 (s, 3H, $CH3CCH_2CH$). IR (cm^{-1}): *ν*(CO) 1968, 1909. FABMS; *m*/*z*: 655 ($[M^+ + H]$, 15), 654 ($[M]^+$, 12), 625 ($[M^+ - CO + H]$, 14), 598 ($[M^+ - 2CO]$, 7), 449 (100), 349 (11), 336 ($[M^+ - 2CO - PPh_3]$, 17), 263 (15), 183 (13), 148 (8). FABMS; *m*/*z*: Mass calc. for $[C_{33}H_{35}FeO_5P]^+$: 598.1572. Found: 598.1552.

4.5.6. (E)-Dicarbonyl[methyl(2,3,4,5-η)-2-carbomethoxy-4-(4-methoxycyclohexadien-1-ylidene)-3-methylbutanoate]triphenylphosphineiron(0) ***5bPPh$_3$***

Experimental procedures and work up were as described in Section 4.5. Experimental details: lithium bis(trimethylsilyl)amide (1.0 ml, 1 M THF, 1.0 mmol). Dimethyl malonate (0.125 g, 0.95 mmol); **4b** (0.300 g, 0.45 mmol). Yield: 0.88 g, 64% based on **4b**. Obtained as a yellow solid as a mixture of two inseparable diastereoisomers in the ratio 1:3, A:B; by NMR. ^{1}H-NMR ($CHCl_3$-*d*, 270 MHz). Diastereoisomer A: δ 6.8–7.8 (m, 15H, Ph), 4.83 (d, 1H, $J = 9.9$ Hz, C=C*H*CHCH$_3$), 3.71 (s, 3H, OCH_3), 3.55 (m, 1H, C3–H), 3.34 (s, 3H, CO_2CH_3), 3.32 (s, 3H, CO_2CH_3), 3.25 (m, 1H, C5–H), 3.24 (d, 1H, $J = 9.2$ Hz, COC*H*CO), 2.85 (ddq, 1H, $J = 6.9$, 9.2, 9.9 Hz, CH_3CHCH), 2.69 (bd, 1H, $J = 17.5$ Hz, C6β–H), 2.22 (m, 2H, C6β–H and C2–H), 0.84 (d, 3H, $J = 6.9$ Hz, CH_3CH). Diastereoisomer B: δ 6.8–7.8 (m, 15H, Ph), 4.88 (d, 1H, $J = 9.9$ Hz, C=C*H*CHCH$_3$), 3.75 (s, 3H, OCH_3), 3.55 (m, 1H, C3–H), 3.39 (s, 3H, CO_2CH_3), 3.33 (d, 1H, $J = 9.2$ Hz, COC*H*CO), 3.26 (s, 3H, CO_2CH_3), 3.25 (m, 1H, C5–H), 2.90 (ddq, 1H, $J = 6.9$, 9.2, 9.9 Hz, CH_3CHCH), 2.69 (bd, 1H, $J = 17.5$ Hz, C6β–H), 2.22 (m, 2H, C6β–H and C2–H), 0.75 (d, 3H, $J = 6.9$ Hz, CH_3CH). IR (cm^{-1}): *ν*(CO) 1977, 1921. FABMS; *m*/*z*: 655 ($[M^+ + H]$, 8), 654 ($[M]^+$, 5), 598 ($[M^+ - 2CO]$, 24), 449 (100), 349 (11), 336 ($[M^+ - 2CO - PPh_3]$, 26), 318 (14), 163 (130, 183 (15), 147 (14). FABMS; *m*/*z*: Mass calc. for $[C_{35}H_{36}FeO_7P]^+$: 655.1548. Found: 655.1563.

4.5.7. (Z)-Dicarbonyl[methyl(2,3,4,5-η)-2-carbomethoxy-4-(4-methoxycyclohexadien-1-ylidene)-4-phenylbutanoate]triphenylphosphineiron(0) ***5dPPh$_3$***

Experimental procedures and work up were as described in Section 4.5. Experimental details: lithium

bis(trimethylsilyl)amide (0.5 ml, 1 M in THF, 0.5 mmol). Diethyl malonate (0.080 g, 0.5 mmol); **4d** (0.200 g, 0.27 mmol). Yield: 1.02 g, 51% based on **4d**. Obtained as a yellow solid. ^{1}H-NMR ($CHCl_3$-*d*, 270 MHz): δ 7.0–7.4 (m, 20H, Ph), 4.16 (bm, 1H, C3–H), 4.06 (dd, 1H, $J = 7.1$, 8.5 Hz, COC*H*CO), 4.00 (q, 4H, $J = 7.6$ Hz, $2 \times CO_2CH_2CH_3$), 3.36 (s, 3H, OCH_3), 3.28 (bs, 1H, C5–H), 3.07 (dd, 1H, $J = 7.1$, 8.3 Hz, C2–H), 2.83 (dd, 1H, $J = 7.1$, 14.4 Hz, PhCC*H*H), 2.76 (m, 1H, C6β–H), 2.75 (dd, 1H, $J = 7.1$, 14.4 Hz, PhCCH*H*), 2.43 (dd, 1H, $J = 5.4$, 17.3 Hz, C6α–H), 1.17 (t, 3H, $J = 7.6$ Hz, $CO_2CH_2CH_3$), 1.15 (t, 3H, $J = 7.6$ Hz, $CO_2CH_2CH_3$). IR (cm^{-1}): *v*(CO) 1970, 1912, 1727, 1594, 1483, 1430, 1262, 845, 757. FABMS; *m*/*z*: 744 ($[M]^+$, 8), 688 ($[M^+ - 2CO]$, 9), 687 ($[M^+ - 2CO - H]$, 20), 585 ($[M^+ -$ malonate], 100), 557 (26), 529 (39), 318 (24), 263 (27), 183(26). FABMS; *m*/*z*: Mass calc. for $[C_{35}H_{30}FeO_3P]^+$: 585.1220. Found: 585.1220.

4.5.8. Tricarbonyl[methyl (2,3,4,5-η)-2-carbomethoxy-2-(4-methoxy-1-(1′-methylethenyl)cyclohexadien-1-yl)ethanoate]iron(0) **6a**

Experimental procedures and work up were as described in Section 4.5. Experimental details: sodium hydride (0.056 g, 60% dispersion in mineral oil, 1.4 mmol). Dimethyl malonate (0.185 g, 1.4 mmol); **2a** (0.300 g, 0.69 mmol). Yield: 0.084 g, 30% based on **2a**. Obtained as a yellow oil. ^{1}H-NMR (C_6H_6-d_6, 270 MHz): δ 5.00 (s, 1H, CH_3C=C*H*H), 4.92 (s, 1H, CH_3C=C*H*H), 4.68 (dd, 1H, $J = 2.3$, 6.9 Hz, C3–H), 3.72 (s, 1H, COC*H*CO), 3.27 (s, 3H, OCH_3), 3.26 (s, 3H, OCH_3), 3.1 (m, 2H, C2–H and C5–H), 2.99 (s, 3H, OCH_3), 2.59 (dd, 1H, $J = 2.6$, 15.5 Hz, C6β–H), 1.87 (dd, 1H, $J = 3.3$, 15.2 Hz, C6α–H), 1.60 (s, 3H, CH_3C=CH_2). IR (cm^{-1}): *v*(CO) 2039, 1962. ^{13}C-NMR (C_6H_6-d_6, 67 MHz): δ 210.7, 168.3, 167.9, 147.1, 140.3, 114.2, 65.0, 60.7, 53.0, 52.3, 52.1, 52.0, 50.0, 37.2, 19.4. The structure was also established by X-ray analysis (Fig. 6, Tables 1 and 3).

4.5.9. Tricarbonyl[methyl (2,3,4,5-η)-2-carbomethoxy-2-(4-methoxy-1-(2′-methylethenyl)cyclohexadien-1-yl)ethanoate]iron(0) **6b**

Experimental procedures and work up were as described in Section 4.5. Experimental details: sodium hydride (0.120 g, 60% dispersion in mineral oil, 3.0 mmol). Dimethyl malonate (0.396 g, 3.0 mmol); **2b** (0.660 g, 1.52 mmol). Yield: 0.287 g, 45% based on **2b**. Obtained as a yellow oil. ^{1}H-NMR ($CHCl_3$-*d*, 270 MHz): δ 5.15 (dq, 1H, $J = 1.7$, 15.3 Hz, C*H*=$CHCH_3$), 5.38 (dq, 1H, $J = 6.9$, 15.3 Hz, CH=C*H*CH_3), 5.02 (dd, 1H, $J = 2.3$, 6.6 Hz, C3–H), 3.80 (s, 1H, COC*H*CO), 3.73 (s, 3H, OCH_3), 3.67 (s, 3H, OCH_3), 3.62 (s, 3H, OCH_3), 3.27 (dt, 1H, $J = 2.6$, 3.3 Hz, C5–H), 3.12 (d, 1H, $J = 6.6$ Hz, C2–H), 2.66 (dd, 1H, $J = 2.6$, 14.8 Hz, C6β–H), 2.21 (dd, 1H, $J = 3.3$, 14.8 Hz, C6α–H), 1.63 (dd, 3H, $J = 1.7$, 7.3 Hz, CH=CHC*H*$_3$). IR (cm^{-1}): *v*(CO) 2054, 1986. EIMS; *m*/*z*: 420 ($[M]^+$, 0.1), 392 ($[M^+ - CO]$, 0.1), 364 ($[M^+ - 2CO]$, 2), 336 ($[M^+ - 3CO]$, 18), 204 (15), 148 (100), 133 (16). Anal. Found: C, 51.6; H, 4.6. Calc. for $C_{18}H_{20}FeO_8$: C, 51.5; H, 4.8%.

4.5.10. Tricarbonyl[methyl (2,3,4,5-η)-2-carbomethoxy-2-(4-methoxy-1-(1′,2′-dimethylethenyl)cyclohexadien-1-yl)ethanoate]iron(0) **6c**

Experimental procedures and work up were as described in Section 4.5. Experimental details: sodium hydride (0.056 g, 60% dispersion in mineral oil, 1.4 mmol). Dimethyl malonate (0.185 g, 1.4 mmol); **2c** (0.300 g, 0.67 mmol). Yield: 0.116 g, 40% based on **2c**. Obtained as a yellow oil. ^{1}H-NMR ($CHCl_3$-*d*, 270 MHz): δ 5.32 (q, 1H, $J = 7.6$ Hz, CH_3C=C*H*CH_3), 5.08 (dd, 1H, $J = 1.4$, 6.3 Hz, 3–H), 3.93 (s, 1H, COC*H*CO), 3.74 (s, 3H, OCH_3), 3.66 (s, 3H, OCH_3), 3.62 (s, 3H, OCH_3), 3.26 m, 2H, C2–H and C5–H), 2.80 (m, 1H, C6β–H), 2.27 (m, 1H, C6α–H), 1.91 (s, 3H, CH_3C=$CHCH_3$), 1.61 (d, 3H, $J = 7.6$ Hz, CH_3C=CHC*H*$_3$). IR (cm^{-1}): *v*(CO) 2043, 1980. EIMS; *m*/*z*: 378 ($[M^+ - 2CO]$, 1), 350 ($[M^+ - 3CO]$, 7), 218 (10), 162 (100), 147 (65). Anal. Found: C, 52.7; H, 5.0. Calc. for $C_{19}H_{20}FeO_8$: C, 52.5; H, 5.1%.

4.5.11. Tricarbonyl[ethyl (2,3,4,5-η)-2-carboethoxy-2-(4-methoxy-1-(1′-phenylethenyl)cyclohexadien-1-yl)ethanoate]iron(0) **6d**

Experimental procedures and work up were as described in Section 4.5. Experimental details: sodium hydride (0.056 g, 60% dispersion in mineral oil, 1.4 mmol). Diethyl malonate (0.224 g, 1.4 mmol); **2d** (0.300 g, 0.67 mmol). Yield: 0.116 g, 40% based on **2d**. Obtained as a yellow oil. ^{1}H-NMR ($CHCl_3$-*d*, 400 MHz): δ 7.35 (3H, m, Ph), 7.10 (m, 2H, Ph), 5.40 (s, 1H, PhC=C*H*H), 5.15 (s, 1H, PhC=CH*H*), 5.00 (dd, 1H, $J = 2.4$, 6.8 Hz, C3–H), 4.13 (q, 4H, $J = 7.2$ Hz, $2 \times CH_3CH_2O$), 3.76 (s, 1H, COC*H*CO), 3.61 (s, 3H, OCH_3), 3.65 (m, 1H, C5–H), 3.36 (d, 1H, $J = 6.8$ Hz, C2–H), 2.83 (bd, 1H, $J = 15.4$ Hz, C6β–H), 2.32 (dd, 1H, $J = 3.18$, 15.4 Hz, C6α–H), 1.10 (q, 6H, $J = 7.20$ Hz, $2 \times CH_3CH_2O$). IR (cm^{-1}): *v*(CO) 2042, 1971. EIMS; *m*/*z*: Mass calc. for $[C_{25}H_{26}FeO_8]^+$: 510.0977. Found: 510.0977.

4.6. General procedure for the addition of organocuprates to **2a**

The appropriate organolithium reagent (four equivalents) was stirred in THF (10 ml) at −30°C and copper bromide dimethyl sulfide complex (two equivalents) was added. The mixture was stirred for a further 1 h until all the copper salt had been consumed. **2a** (one equivalent) was added as a solid in one portion and the mixture was stirred for a further 2 h at −30°C fol-

lowed by the addition of saturated aqueous ammonium chloride solution. The mixture was extracted with diethyl ether (3 × 50 ml) and the combined extracts were washed with water (2 × 50 ml) and brine (1 × 50 ml). The solution was dried over magnesium sulfate and the solvent removed in vacuo. The residue was purified by column chromatography on silica gel to afford the required compounds as yellow oils.

4.6.1. (1E)-Tricarbonyl[(2,3,4,5-η)-4-methoxy-1-(1-methylpropylidene)cyclohexadiene]iron(0) **8a**

Experimental procedures and work up were as described in Section 4.6. Experimental details: dimethylcuprate (2.0 mmol); **2a** (0.250 g, 0.57 mmol). Yield: 0.135 g, 78% based on **2a**. Obtained as a yellow oil. ^{1}H-NMR ($CHCl_3$-*d*, 270 MHz): δ 5.05 (dd, 1H, $J = 2.6$, 6.6 Hz, C3–H), 3.58 (s, 3H, OCH_3), 3.46 (m, 1H, C5–H), 3.36 (d, 1H, $J = 6.9$ Hz, C2–H), 2.36 (db, 1H, $J = 14.4$ Hz, C6β–H), 2.17 (bd, 1H, 14.4 Hz, C6α–H), 1.78 (dq, 1H, $J = 7.6$, 13.5 Hz, CH_2CH_3), 1.59 (t, 3H, $J = 1.3$ Hz, CH_3CCH_2), 0.81 (t, 3H, $J = 7.6$ Hz, CH_2CH_3). ^{1}H-NMR ($CHCl_3$-*d*, 270 MHz, n.O.e.): irradiation at δ 1.59 (t, 3H, $J = 1.3$ Hz, CH_3CCH_2). Observed n.O.e.: δ 3.36 (3.5%, d, 1H, $J = 6.9$ Hz, C2–H). IR (cm^{-1}): ν(CO) 2043, 1978, 1968. EIMS; *m*/*z*: 304 ([M]$^+$, 31), 276 ([M$^+$ − CO], 49), 248 ([M$^+$ − 2CO], 25), 220 (95), 218 (100), 216 (43), 178 (44). EIMS; *m*/*z*: Mass calc. for $[C_{14}H_{16}O_4Fe]^+$: 304.0398. Found: 304.0398.

4.6.2. (1E)-Tricarbonyl[(2,3,4,5-η)-4-methoxy-1-(1-methylhexylidene)cyclohexadiene]iron(0) **8b**

Experimental procedures and work up were as described in Section 4.6. Experimental details: dimethylcuprate (2.0 mmol); **2a** (0.230 g, 0.53 mmol). Yield: 0.128 g, 70% based on **2a**. Obtained as a yellow oil. ^{1}H-NMR ($CHCl_3$-*d*, 270 MHz): δ 5.10 (dd, 1H, $J = 2.4$, 6.6 Hz, C3–H), 3.64 (s, 3H, OCH_3), 3.49 (m, 1H, C5–H), 3.43 (d, 1H, $J = 6.6$ Hz, C2–H), 2.35 (m, 1H, C6β–H), 1.80 (m, 1H, C6α–H), 1.65 (t, 3H, $J = 1.3$ Hz, CH_3CCH_2), 1.2 (m, 11H, $CH_2CH_2CH_2CH_2CH_3$). ^{1}H-NMR ($CHCl_3$-*d*, 270 MHz, n.O.e.): irradiation at δ 1.65 (t, 3H, $J = 1.3$ Hz, CH_3CCH_2). Observed n.O.e.: δ 3.42 (4.0%, d, 1H, $J = 6.6$ Hz, C2–H). ^{13}C-NMR ($CHCl_3$-*d*, 67 MHz): δ 211.3 (M*C*O), 139.4 (C4), 129.0 (C1), 125.6 (CH_3CCH_2), 65.6 (C3), 54.4 (OCH_3), 52.6 (C2), 52.4 (C5), 35.0 (C6), 31.8 (CH_3CCH_2), 29.4 ($CH_3CCH_2CH_2$), 27.1 ($CH_3CCH_2CH_2CH_2$), 22.6 ($CH_3CCH_2CH_2CH_2CH_2$), 17.3 (CH_3CCH_2), 13.9 (CH_2CH_3). IR (cm^{-1}): ν(CO) 2041, 1970. Anal. Found: C, 59.1; H, 6.4. Calc. for $C_{17}H_{22}O_4Fe$: C, 59.0; H, 6.4%. EIMS; *m*/*z*: 346 ([M]$^+$, 2), 318 ([M$^+$ − CO], 26), 290 ([M$^+$ − 2CO], 9), 262 ([M$^+$ − 3CO], 36), 190 (30), 135 (100).

4.6.3. (1E)-Tricarbonyl[(2,3,4,5-η)-4-methoxy-1-(1-methyl-2-phenyl)ethylidene)cyclohexadiene]iron(0) **8c**

Experimental procedures and work up were as described in Section 4.6. Experimental details: diphenylcuprate (4.60 mmol); **2a** (0.500 g, 1.15 mmol). Yield: 0.282 g, 67% based on **2a**. Obtained as a yellow oil. ^{1}H-NMR ($CHCl_3$-*d*, 270 MHz): δ 7.15 (m, 5H, ArH), 5.15 (dd, 1H, $J = 2.6$, 6.9 Hz, C3–H), 3.67 (s, 3H, OCH_3), 3.55 (m, 1H, C5–H), 3.46 (d, 1H, $J = 6.6$ Hz, C2–H), 3.27 (d, 1H, $J = 14.8$ Hz, CH_2Ph), 3.05 (d, 1H, $J = 14.8$ Hz, CH_2Ph), 2.60 (bd, 1H, $J = 17.2$ Hz, C6β–H), 2.40 (bd, 1H, $J = 17.2$ Hz, C6α–H), 1.60 (s, 3H, CH_3C). ^{1}H-NMR ($CHCl_3$-*d*, 270 MHz, n.O.e.): irradiation at δ 1.60 (s, 3H, CH_3C). Observed n.O.e.: δ 3.46 (4.5%, d, 1H, $J = 6.6$ Hz, C2–H). IR (cm^{-1}): ν(CO) 2040, 1965. Anal. Found: C, 62.6; H, 4.8. Calc. for $C_{19}H_{18}O_4Fe$: C, 62.3; H, 4.9%. EIMS; *m*/*z*: 338 ([M$^+$ − CO], 1), 310 ([M$^+$ − 2CO], 1), 282 ([M$^+$ − 3CO], 8), 224 (13), 204 (13), 148 (36), 135 (100).

4.7. Formation of cations **9**

4.7.1. Tricarbonyl[(1,2,3,4,5-η)-4-methoxy-1-(1-methylpropyl)cyclohexdienyl]iron(1 +) hexafluorophosphate(1 −) **9a**

Experimental procedures and work up were as described in Section 4.2. Experimental details: **8a** (0.120 g, 0.39 mmol). Yield: 0.127 g, 72%. Recovered as a single diastereoisomer as a pale yellow solid. ^{1}H-NMR (CH_3CN-d_3, 270 MHz): δ 6.80 (dd, 1H, $J = 2.3$, 5.9 Hz, C3–H), 5.56 (d, 1H, $J = 5.9$ Hz, C2–H), 3.90 (d, 1H, $J = 5.9$ Hz, C5–H), 3.78 (s, 3H, OCH_3), 3.03 (dd, 1H, $J = 6.3$, 15.5 Hz, C6β–H), 2.25 (bd, 1H, $J = 15.5$ Hz, C6α–H), 1.89 (sextet, 1H, $J = 6.9$ Hz, CH_3CHCH_2), 1.48 (m, 2H, $CHCH_2CH_3$), 1.18 (d, 3H, $J = 6.9$ Hz, CH_3CH), 0.87 (t, 3H, $J = 7.3$ Hz, CH_2CH_3). ^{13}C-NMR (CH_3CN-d_3, 67 MHz): δ 150.7 (C4), 100.2 (C1), 94.9 (C2), 72.5 (C3), 58.0 (OCH_3), 43.2 (C5), 42.6 (CH_3CHCH_2), 29.8 (C6), 27.1 ($CHCH_2CH_3$), 19.06 (CH_3CH), 11.9 ($CHCH_2CH_3$). IR (cm^{-1}): ν(CO) 2102, 2057. Anal. Found: C, 37.5; H, 3.7. Calc. for $C_{14}H_{17}O_4FePF_6$: C, 37.4; H, 3.8%. EIMS; *m*/*z*: 304 ([M$^+$ − H], 3), 277 ([M$^+$ − CO], 4), 276 ([M$^+$ − CO − H], 23), 249 ([M$^+$ − 2CO], 2), 248 ([M$^+$ − 2CO − H], 14), 221 ([M$^+$ − 3CO], 10), 220 ([M$^+$ − 3CO − H], 59), 218 (40), 135 (100).

4.7.2. Tricarbonyl[(1,2,3,4,5-η)-4-methoxy-1-(1-methylhexyl)cyclohexdienyl]iron(1 +) hexafluorophosphate(1 −) **9b**

Experimental procedures and work up were as described in Section 4.2. Experimental details: **8b** (0.121 g, 0.35 mmol). Yield: 0.100 g, 66%. Recovered as a single diastereoisomer as a pale yellow solid. ^{1}H-NMR (acetone-d_6, 270 MHz): δ 6.80 (br, 1H, C3–H), 5.56 (br, 1H, C2–H), 3.90 (br, 1H, C5–H), 3.79 (s, 3H, OCH_3),

3.01 (br, 1H, C6β–H), 2.50 (m, 1H, CH_3CHCH_2), 2.28 (br, 1H, C6α–H), 0.9–1.4 (m, 14H, CH_3CHCH_2-$CH_2CH_2CH_2CH_3$). ^{13}C-NMR (acetone-d_6, 67 MHz): δ 213.0 (CO), 148.2 (C4), 98.6 (C1), 92.2 (C2), 69.9 (C3), 55.5 (OCH_3), 38.4 (C5), 38.2 (CH_3CHCH_2), 31.5 (C6), 29.5 (CH_3CHCH_2), 27.5 ($CHCH_2CH_2$), 24.7 ($CHCH_2$-CH_2CH_2), 20.4 (CH_3CH), 16.9 ($CHCH_2CH_2CH_2CH_2$), 11.5 (CH_2CH_3). IR (cm^{-1}): ν(CO) 2107, 2057. EIMS; m/z: 347 ([$M^+ + H$)], 346 ([M)$^+$], 318 ([$M^+ + H -$ CO], 4), 290 ([$M^+ - 2CO$)], 262 ([$M^+ - 3CO$)], 135 (100). EIMS; m/z: Mass calc. for [$C_{17}H_{23}O_4Fe$]$^+$: 347.095. Found: 347.095.

*4.7.3. Tricarbonyl[(1,2,3,4,5-η)-1-(1-benzylethyl)-4-methoxycyclohexdienyl]iron(1 +) hexafluorophosphate(1 −) **9c***

Experimental procedures and work up were as described in Section 4.2. Experimental details: **8c** (0.105 g, 0.29 mmol). Yield: 0.093 g, 65%. Recovered as a single diastereoisomer as a pale yellow solid. ^{1}H-NMR (CH_3CN-d_3, 270 MHz): δ 7.23 (m, 5H, ArH), 7.09 (dd, 1H, $J = 2.3$, 5.9 Hz, C3–H), 5.83 (d, 1H, $J = 5.9$ Hz, C2–H), 4.31 (d, 1H, $J = 6.3$ Hz, C5–H), 3.96 (s, 3H, OCH_3), 3.36 (dd, 1H, $J = 6.3$, 15.2 Hz, C6β–H), 2.65 (d, 2H, $J = 7.1$ Hz, $CHCH_2Ph$), 2.51 (bd, 1H, $J = 15.2$ Hz, C6α–H), 2.43 (m, 1H, CH_3CHCH_2), 1.27 (d, 3H, $J = 6.6$ Hz, CH_3CH). ^{13}C-NMR (CH_3CN-d_3, 67 MHz): δ 150.8 (C4), 139.4, 129.8, 129.4, 127.5 (ArC), 98.3 (C1), 95.5 (C2), 72.4 (C3), 58.0 (OCH_3), 43.4 (C5), 43.1 (CH_3CHCH_2), 40.4 (CH_3CHCH_2), 29.6 (C6), 19.3 (CH_3CH). IR (cm^{-1}): ν(CO) 2107, 2057. EIMS; m/z: 339 ([$M^+ + H - CO$)], 310 ([$M^+ + H - 2CO$)], 282 ([$M^+ + H - 3CO$)], 135 (100). CIMS m/z: Mass calc. for [$C_{18}H_{20}O_3Fe$]$^+$: 339.068. Found: 339.068.

5. X-ray data collection

5.1. Crystallography

Crystallographic data for compounds **2a, 2d, 4b** and **6a** are summarised in Table 3.

Data collections were conducted on a CAD4 automatic four-circle diffractometer at ambient temperature using Mo–K_α radiation ($\lambda = 0.71069$ Å) for **2a, 2d** and **4b** and on a Siemens P4 for **6a**. Full-matrix anisotropic refinement was implemented in the final least-squares cycles throughout. Four of the fluorines in the PF_6 anion were seen to be disorder in the ratio 3:2 with their primed counterparts in compound **2a**. Hydrogens were included at calculated positions as appropriate, with the exception of H4, H6 and H7 in **2a**, H211, H231, H241, H281 and H291 in **4b**, and H4, H6 and H7 in **2d**. These hydrogens were readily located in their respective penultimate difference Fourier maps and freely refined.

6. Supplementary material

Crystallographic data for the structural analysis have been deposited with the Cambridge Crystallographic Data Centre, CCDC nos. 154839 for compound **2a**, 154841 for compound **2d**, 154840 for compound **4b** and 155022 for compound **6a**. Copies of this information may be obtained free of charge from The Director, CCDC, 12 Union Road, Cambridge CB2 1EZ, UK (Fax: +44-1223-336033; e-mail: deposit@ccdc.cam.ac.uk or www:http://www.ccdc.cam.ac.uk).

Acknowledgements

This work was supported by EPSRC and Parke–Davis (financial support to R.D.A.H.). We thank the EPSRC Mass Spectrometry Centre (Swansea) for FAB and high-resolution mass spectrometric measurements. Microanalyses and low-resolution mass spectrometric measurements were made by Mr I. Saunders, University of East Anglia, Norwich.

References

[1] (a) R.D.A. Hudson, B.M. Foxman, M. Rosenblum, Organometallics 18 (1999) 4098. (b) R.D.A. Hudson, B.M. Foxman, M. Rosenblum, Organometallics 19 (2000) 469.
[2] E.W. Abel, F.G.A. Stone, G. Wilkinson (Eds.), Comprehensive Organometallic Chemistry 11, vols. 5–9, Pergamon Press/Elsevier Science, Oxford, 1995 (for applications in synthesis, see vol. 12).
[3] (a) M. Franck-Neumann, L. Meisch-Gross, C. Gateau, Tetrahedron Lett. 40 (1999) 2829. (b) T.J. Benvegnu, L.J. Toupet, R.L. Grée, Tetrahedron 52 (1996) 11 811. (c) B. Dasgupta, W.A. Donaldson, Tetrahedron: Asymmetry 9 (1998) 3781.
[4] (a) B.M.R. Bandara, A.J. Birch, L.F. Kelly, J. Org. Chem. 49 (1984) 2496. (b) A.J. Birch, L.F. Kelly, D.V. Weerasuria, J. Org. Chem. 53 (1988) 278. (c) A.J. Pearson, A. Alimardanov, A.A. Pinkerton, D.M. Fouchard, K. Kirschbaum, Tetrahedron Lett. 39 (1998) 5919. (d) H.-J. Knölker, E. Baum, T. Hopfmann, Tetrahedron 55 (1999) 10 391. (e) H.-J. Knölker, W. Fröhner, Tetrahedron Lett. 40 (1999) 6915.
[5] G.R. Stephenson (Ed.), Advanced Asymmetric Synthesis, Blackie/Chapman & Hall, London, 1996, pp. 319–320.
[6] G.R. Stephenson, H. Finch, D.A. Owen, S. Swanson, Tetrahedron 49 (1993) 5649.
[7] E.J. Sandoe, G.R. Stephenson, S. Swanson, Tetrahedron Lett. 37 (1996) 6283.
[8] S.T. Astley, G.R. Stephenson, Synlett (1992) 507.
[9] (a) G.R. Stephenson, I.M. Palotai, W.J. Ross, D.E. Tupper, J. Organomet. Chem. 364 (1991) C11. (b) G.R. Stephenson, I.M. Palotai, W.J. Ross, D.E. Tupper, Synlett (1991) 586. (c) M. Tinkl, PhD Thesis, University of East Anglia, Norwich, 1995.
[10] D.A. Owen, G.R. Stephenson, H. Finch, S. Swanson, Tetrahedron Lett. 30 (1998) 2607.
[11] N. Genco, D. Marten, S. Raghu, M. Rosenblum, J. Am. Chem. Soc. 98 (1976) 848. For further examples of Rosenblum's cationic Fp complexes with alkenes and their regio- and stereochemical reactions with nucleophiles see W. Zhen, K.-H Chu, M. Rosenblum, J. Org. Chem. 62 (1997) 3344 and references cited therein.

[12] P. Lennon, A.M. Rosan, M. Rosenblum, J. Am. Chem. Soc. 99 (1977) 8426.
[13] N. Genco, D. Marten, S. Raghu, M. Rosenblum, J. Am. Chem. Soc. 98 (1976) 848.
[14] P. McArdle, J. Appl. Crystallogr. 28 (1995) 65.
[15] (a) M.F. Semmelhack, H.T. Hall Jr., R. Farina, M. Yoshifuji, G. Clark, T. Bargar, K. Hirotsu, J. Clardy, J. Am. Chem. Soc. 101 (1979) 3535. (b) N.A. Bailey, E.H. Blunt, G. Fairhurst, C. White, J. Chem. Soc. Dalton Trans. (1980) 829. (c) M. Bottrill, M. Green, E. O'Brien, L.E. Smart, P. Woodward, J. Chem. Soc. Dalton Trans. (1980) 292. (d) B. Etermadi, D.S. Moss, R.A. Palmer, J. Inorg. Nucl. Chem. 43 (1981) 1997. (e) P. Janse Van Nuuren, R.J. Fletterich, J. Meinwald, R.E. Hughes, J. Am. Chem. Soc. 93 (1971) 4394.
[16] J. March, Advanced Organic Chemistry, 4th ed., Wiley, New York, 1992 (pp. 19–21).
[17] O. Eisenstein, W.M. Butler, A.J. Pearson, Organometallics 3 (1984) 1150.
[18] (a) G.R. Stephenson, M. Voyle, S. Williams, Tetrahedron Lett. 31 (1990) 3979. (b) Preliminary communication: R.D.A. Hudson, S.A. Osborne, E. Roberts, D.G. Smyth, G.R.Stephenson, Tetrahedron Lett. 37 (1996) 9009. (c) R.D.A. Hudson, S.A. Osborne, G.R.Stephenson, Tetrahedron 53 (1997) 4095.
[19] (a) A.J. Pearson, P.R. Raithby, J. Chem. Soc. Dalton Trans. (1981) 884. (b) J.A.D. Jeffreys, C. Metters, J. Chem. Soc. Dalton Trans. (1977) 729.
[20] A.J. Birch, P.E. Cross, J. Lewis, D.A. White, S.B. Wild, J. Chem. Soc. A. (1968) 332.
[21] C.E. Anson, R.D.A. Hudson, D.G. Smyth, G.R. Stephenson, Appl. Organomet. Chem. 15 (2001) 16.
[22] Preliminary communication: C.E. Anson, R.D.A. Hudson, S.A. Osborne, G.R. Stephenson, Tetrahedron Lett. 39 (1998) 7603.
[23] D. Seebach, H. Neuman, Terahedron Lett. 52 (1976) 4839.
[24] A.J. Birch, L.F. Kelly, J. Organomet. Chem. 286 (1985) C5.